



HAL
open science

A Large Committed Long-Term Sink of Carbon due to Vegetation Dynamics

T. A. M. Pugh, C. D. Jones, C. Huntingford, C. Burton, A. Arneth, V. Brovkin, Philippe Ciais, M. Lomas, E. Robertson, S. L. Piao, et al.

► **To cite this version:**

T. A. M. Pugh, C. D. Jones, C. Huntingford, C. Burton, A. Arneth, et al.. A Large Committed Long-Term Sink of Carbon due to Vegetation Dynamics. *Earth's Future*, 2018, 6, pp.1413-1432. 10.1029/2018EF000935 . insu-03721859

HAL Id: insu-03721859

<https://insu.hal.science/insu-03721859v1>

Submitted on 16 Jul 2022

HAL is a multi-disciplinary open access archive for the deposit and dissemination of scientific research documents, whether they are published or not. The documents may come from teaching and research institutions in France or abroad, or from public or private research centers.

L'archive ouverte pluridisciplinaire **HAL**, est destinée au dépôt et à la diffusion de documents scientifiques de niveau recherche, publiés ou non, émanant des établissements d'enseignement et de recherche français ou étrangers, des laboratoires publics ou privés.

Copyright



Earth's Future

RESEARCH ARTICLE

10.1029/2018EF000935

Key Points:

- Terrestrial vegetation composition and carbon storage continue to change very substantially after stabilization of climate
- Uncertainty in this committed carbon uptake is of the order of several hundred Pg C, complicating emission budget calculations
- Vegetation dynamics need to be more routinely represented in the coupled Earth System Models used to make climate projections

Supporting Information:

- Supporting Information S1
- Data Set S2

Correspondence to:

T. A. M. Pugh,
t.a.m.pugh@bham.ac.uk

Citation:

Pugh, T. A. M., Jones, C. D., Huntingford, C., Burton, C., Arneth, A., Brovkin, V., et al. (2018). A large committed long-term sink of carbon due to vegetation dynamics. *Earth's Future*, 6, 1413–1432. <https://doi.org/10.1029/2018EF000935>






Received 1 AUG 2017

Accepted 9 SEP 2018

Accepted article online 12 SEP 2018

Published online 4 OCT 2018

A Large Committed Long-Term Sink of Carbon due to Vegetation Dynamics

T. A. M. Pugh^{1,2} , C. D. Jones³ , C. Huntingford⁴, C. Burton³ , A. Arneth², V. Brovkin⁵ , P. Ciais⁶, M. Lomas⁷, E. Robertson³ , S. L. Piao⁸ , and S. Sitch⁹ 

¹School of Geography, Earth and Environmental Sciences and Birmingham Institute of Forest Research, University of Birmingham, Birmingham, UK, ²Karlsruhe Institute of Technology, Institute of Atmospheric Environmental Research (IMK-IFU), Garmisch-Partenkirchen, Germany, ³Met Office Hadley Centre, Exeter, UK, ⁴Centre for Ecology and Hydrology, Wallingford, UK, ⁵Max Planck Institute for Meteorology, Hamburg, Germany, ⁶Laboratoire des Sciences du Climat et de l'Environnement, Gif-Sur-Yvette, France, ⁷Centre for Terrestrial Carbon Dynamics, University of Sheffield, Sheffield, UK, ⁸Department of Ecology, College of Urban and Environmental Sciences, Peking University, Beijing, China, ⁹Geography College of Life and Environmental Sciences, University of Exeter, Exeter, UK

Abstract The terrestrial biosphere shows substantial inertia in its response to environmental change. Hence, assessments of transient changes in ecosystem properties to 2100 do not capture the full magnitude of the response realized once ecosystems reach an effective equilibrium with the changed environmental boundary conditions. This equilibrium state can be termed the *committed state*, in contrast to a *transient state* in which the ecosystem is in disequilibrium. The difference in ecosystem properties between the transient and committed states represents the *committed change* yet to be realized. Here an ensemble of dynamic global vegetation model simulations was used to assess the changes in tree cover and carbon storage for a variety of committed states, relative to a preindustrial baseline, and to attribute the drivers of uncertainty. Using a subset of simulations, the committed changes in these variables post-2100, assuming climate stabilization, were calculated. The results show large committed changes in tree cover and carbon storage, with model disparities driven by residence time in the tropics, and residence time and productivity in the boreal. Large changes remain ongoing well beyond the end of the 21st century. In boreal ecosystems, the simulated increase in vegetation carbon storage above preindustrial levels was 20–95 Pg C at 2 K of warming, and 45–201 Pg C at 5 K, of which 38–155 Pg C was due to expansion in tree cover. Reducing the large uncertainties in long-term commitment and rate-of-change of terrestrial carbon uptake will be crucial for assessments of emissions budgets consistent with limiting climate change.

Plain Language Summary Changes in climate and atmospheric carbon dioxide concentration affect ecosystems. One result of these effects, projected by most vegetation models, is that the global land biosphere is expected to continue to provide a net uptake of carbon dioxide throughout the 21st century. Characterizing this is important for policy, as it influences the amount of carbon dioxide emissions reductions needed to limit global warming. However, the effects of such environmental changes on land ecosystems are not all realized instantly. Ecosystems may continue to react to a change in their wider environment for decades or centuries after that change has occurred. These delayed reactions are termed the *committed change*. We found widespread agreement among multiple vegetation models that land in the far north will continue to take up a large amount of carbon in the long-term, as a result of committed responses to climate change and carbon dioxide increases. The magnitude of uptake varied between simulations and was partially driven by an advance of the northern treeline. A less consistent model response was found in the tropics. The large amount of carbon involved, and associated climate policy implications, illustrates the benefits of further measurements leading to more accurate vegetation model calibration.

1. Introduction

Terrestrial ecosystems respond to changes in the environment in which they exist, but they do so with a substantial lag. This fact has long been acknowledged (e.g., Smith & Shugart, 1993), leading eventually to the development of dynamic global vegetation models (DGVMs) to explore dynamic changes in global terrestrial ecosystem state and function under different environmental conditions (Cramer et al., 2001). Such DGVMs have shown success in reproducing the main features of current global vegetation (e.g., Hickler et al., 2006; Piao et al., 2013; Sitch et al., 2015, 2008; Zhu et al., 2015) and are widely used to simulate changes in

©2018. The Authors.

This is an open access article under the terms of the Creative Commons Attribution License, which permits use, distribution and reproduction in any medium, provided the original work is properly cited.

the carbon stocks and fluxes of the terrestrial biosphere, including as part of some Earth System Models (ESMs; Dunne et al., 2013; Giorgetta et al., 2013; Martin et al., 2011). But the overwhelming focus of studies on a time horizon of 2100 means that the full consequences of environmental change for the global terrestrial biosphere have only seen limited consideration to date. Jones et al. (2009) demonstrated that the projected tree cover in transient simulations with evolving climate and atmospheric CO₂ mixing ratio ([CO₂]) differed substantially from the projected equilibrium state of tree cover with the same environmental forcings. Using the HadCM3LC ESM, they found that the equilibrium changes in vegetation cover implied by a change in environmental forcing greatly exceeded the transient changes simulated during the 21st century. The difference in ecosystem properties between this equilibrium or *committed* state (termed *capacity* by Luo et al., 2017) and a transient state in disequilibrium can be termed the *committed change* yet to be realized (termed *potential* by Luo et al., 2017), assuming that environmental boundary conditions remain constant. The term *equilibrium* herein refers to a broadly constant state over a large area and multidecadal timescales. Large changes in ecosystem properties going beyond typical time horizons would have substantial implications for assessing the long-term impacts of even relatively moderate climate change. It also implies that following any stabilization of climate and [CO₂], there will be a further period during which terrestrial ecosystem changes occur, which will of themselves influence the final climate state. Transient ecosystem states at the point of cessation of climate change will not immediately reveal the committed ecosystem state in equilibrium with any stabilized climate.

Vegetation biomass contains circa 500 Pg C globally (e.g., Avitabile et al., 2016; Thurner et al., 2014), while the productivity and turnover rate of vegetation control the input of carbon to soil and thus influence soil carbon stocks and respiration fluxes. Soil carbon stocks also show a long lag in response to changes in inputs, especially in cold regions (simulated in Pugh et al., 2015). In response to elevated [CO₂] and higher temperatures under climate change, early biogeography models, which assumed equilibrium of vegetation with climate, projected large northward expansions of forest biomes and potential losses of biomass in the tropics (Neilson et al., 1998). A handful of recent studies have also used climate similarity methods to project equilibrium future vegetation distributions and biomass with similar results (Koven, 2013; Zeng et al., 2013). A limitation of equilibrium approaches, however, is that they cannot assign any time frames to the simulated changes in vegetation composition and carbon storage.

Three DGVM studies have included quantification of committed vegetation carbon effects including some information on rates of change. Sitch et al. (2008) found further increases in global vegetation biomass and losses of soil carbon after climate stabilization, albeit with large regional variation, in a study with the LPJ DGVM under a strong climate change scenario. Using the TRIFFID DGVM, Huntingford et al. (2013) found often-substantial differences in tropical carbon stocks between transient projections for 2100 under strong climate change and committed equilibrium stocks under climate and [CO₂] held constant at 2100 levels. Likewise, Port et al. (2012) simulated continued global uptake of carbon by the terrestrial biosphere using Max-Planck-Institute Earth System Model (MPI-ESM) following stabilization of atmospheric radiative forcing from 2100 on. These changes in carbon storage resulted both from changes in carbon storage within existing ecosystems and from vegetation dynamics leading to a change in land-cover type.

However, the committed state of terrestrial vegetation cover and carbon storage has not undergone a concerted investigation. Given the finding that climate-driven changes in land cover are likely to be of equivalent size to those of the now widely considered anthropogenic land-use change, especially over long timescales and under scenarios with strong increases in radiative forcing (Davies-Barnard et al., 2015), this is a very notable omission. Furthermore, uncertainty in future ecosystem carbon stocks under a given radiative forcing scenario is known to be driven by both uncertainties in climate response and by uncertainties in vegetation model structure and parameterization (Friend et al., 2014; Jones et al., 2013). Simulations of committed ecosystem state offer the opportunity to assess the size and relative importance of such uncertainties by evaluating their effect on the ultimate controls of carbon stocks, equilibrium productivity, and turnover time, without the confounding factor of differences in transient rates of change.

To design bespoke numerical experiments for a wide community of models to perform is a very large and intensive process, expensive in both human and computational resources (see, e.g., Eyring et al., 2016). Instead, the analysis herein draws on a range of existing results to assess the existence of any consensus

on the evolution of terrestrial vegetation cover and carbon storage as a result of global environmental change. These sets of simulations were performed at different times, by different modeling groups, and for different projects to address different aspects of committed ecosystem changes. They are assembled here into a large *ensemble of opportunity* in order to synthesize this useful information to address the relative roles of different uncertainty contributions to future ecosystem commitments. All but one of the DGVMs included vegetation dynamics, which is defined here as the simulation of change in the relative cover of plant functional types as environmental boundary conditions change.

Many factors influence future terrestrial carbon stores, including the transient response of primary productivity and respiration in response to changes in $[\text{CO}_2]$ and climate. Anthropogenic land use is also a major driver, as is the potential of thawed carbon in permafrost to be released to the atmosphere, the latter missing from most DGVMs and ESMs. This analysis presents another, often overlooked, process also missing from many ESMs: committed changes due to vegetation dynamics. Specifically, the analysis aims the following:

1. Provide a synthesis of differences in tree cover and carbon storage between preindustrial and committed states under a range of climates and $[\text{CO}_2]$ from multiple DGVMs.
2. Attribute uncertainty in these states between DGVM structural/parameter uncertainty and uncertainty in the driving climate.
3. Assess the likely magnitude and direction of committed changes in biospheric carbon stocks post-2100 due to prior climate change.

2. Materials and Methods

The ensemble used in this analysis comprises results from $N = 63$ simulations (Figure 1), consisting of the following:

1. Thirty off-line vegetation simulations (previously unpublished) from five different DGVMs (HyLand, LPJ, ORCHIDEE, SDGVM, and TRIFFID, respectively, henceforth referred to as HYL, LPJ, ORC, SHE, and TRI for brevity when referring to these simulations) forced by HadCM3LC climate data, spun-up directly to equilibrium (committed) state for multiple stabilization levels of global temperatures and $[\text{CO}_2]$ (blue squares in Figure 1). Henceforth termed the *DGVM ensemble*.
2. Twenty-two off-line vegetation simulations by the TRIFFID DGVM forced by different climate patterns from the Coupled Model Intercomparison Project Phase 3 (CMIP3) multimodel archive, but following the same climate-forcing scenario (Huntingford et al., 2013; black stars in Figure 1). Simulations were run under transient forcings from 1850 to 2100 and then run to equilibrium under fixed 2100 forcing. Henceforth termed the *climate ensemble*.
3. Ten fully coupled ESM simulations (eight from the HadCM3LC model published in Jones et al., 2009; black triangles in Figure 1, and one each from Hadley Centre Global Environmental Model version 2 Earth System (HadGEM2-ES) and MPI-ESM, previously unpublished; blue and magenta circles in Figure 1) and one further off-line DGVM simulation (LPJ-GUESS forced by climate from the ESM EC-Earth, previously unpublished; red circle in Figure 1). Simulations were run under transient forcings from a variety of pre-industrial base years to 2100 and then run to equilibrium under fixed 2100 forcing. Henceforth termed the *ESM ensemble*.

These simulations allow us to investigate the relative roles of and uncertainty arising from using different climate projections (global mean temperature rise above the preindustrial period, ΔT from 0 to 6.8 K), using different climate forcing scenarios ($[\text{CO}_2]$ ranges from 286 to 1,025 ppmv) and from using different DGVMs. The DGVM ensemble contains five DGVMs, but in total, across all the subensembles, results from 10 different DGVMs are synthesized herein ($N_{\text{DGVM}} = 10$), including four different realizations/versions of the TRIFFID DGVM, either stand-alone or operated within HadCM3LC/HadGEM2-ES (see Appendix A). A subset of results comprising the climate ensemble and the ESM ensemble includes both transient and equilibrium simulations ($N = 33$, $N_{\text{DGVM}} = 5$) and can be used to quantify the size of the unrealized change post climate stabilization at 2100. As these collections of data stem from different experimental designs and scenarios, they are primarily explored here in phase space instead of through time. The spread of results across the climate ensemble, which uses a single DGVM and $[\text{CO}_2]$, allows to investigate uncertainty due to the climate response of the driving global climate models alone (see Figure 1), while the DGVM ensemble, for which $[\text{CO}_2]$ also varies,

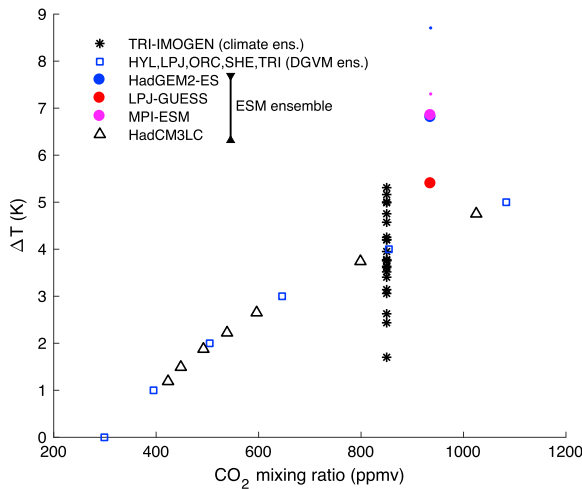


Figure 1. Summary of simulations used in this analysis, displayed as a function of atmospheric CO₂ mixing ratio and the associated global mean temperature rise above preindustrial (ΔT) under which the models were run to their committed state. For the HadGEM2-ES and MPI-ESM simulations, radiative forcing was fixed, but the climate was allowed to continue to evolve after this point; thus, the large dots illustrate the ΔT at the point at which forcing was fixed (year 2100) and the small dots the ΔT at the committed state. Note that the large dot for MPI-ESM overlays that for HadGEM2-ES.

allows to assess the combined uncertainty due to both climate and future radiative forcing (i.e., [CO₂]) scenario. Assessing the DGVM ensemble across a given ΔT window allows to assess uncertainty across model structure and parameter combinations. Each model/scenario/climate realization is treated to be as likely as each of the others.

For all these simulations the DGVM or ESM used was run to quasi-equilibrium (effective equilibrium; in some DGVMs accounting for inter-annual variability; see Appendix A) of the terrestrial biosphere component under fixed climate and [CO₂] forcing, either directly (DGVM ensemble), or following an initial simulation under transient forcings (climate ensemble and ESM ensemble). As DGVMs such as those used here do not show sensitivity of final quasi-equilibrium states to initial conditions (e.g., Clark et al., 2011), these different protocols are compatible. The treatment of land-use change varies between the simulations and is summarized in Table 1. For consistency, the three models that accounted for anthropogenic land-cover change (HadGEM2-ES, MPI-ESM, and LPJ-GUESS) are excluded from the uncertainty analysis in section 3.3. The ensemble also integrates over fully coupled climate-land simulations and off-line land simulations. The former will allow biophysical feedback from any land cover change onto the driving climate, as well as including some lagged climate warming due to, for example, ocean processes. The 2100 and committed global mean temperatures for HadGEM2-ES and MPI-ESM are shown with small and large dots, respectively, in Figure 1. This feedback will be explicitly absent in the off-line simulations. No attempt is made to correct for any of these effects in the results, but the differences in the processes operat-

ing are considered in the interpretation. Further, details of the setup of previously unpublished simulations are given in Appendix A. Tree cover fraction is calculated relative to global land area excluding Antarctica. Results are presented globally and from three latitude bands: tropical (23°S–23°N), temperate (23–55°N), and boreal (>55°N). Given the wide variation in representation of plant types between the DGVMs, within the context of this analysis, *vegetation dynamics* is used to refer specifically to changes in land-cover type between tree cover and low vegetation, such as grasses and shrubs, unless otherwise stated.

The concept of fixing forcing at 2100 is an artificial one, but one that allows attribution of committed changes in the biosphere. It is recognized that long-term climate feedbacks mean that efforts to cease emissions of radiatively active gases will not lead to an immediate stabilization of climate. Indeed, the lags in climate stabilization induced by the oceans are known to be many decades or even centuries (Hare & Meinshausen,

Table 1
Simulation Setups

Ensemble	DGVM	Land-use forcing	Dynamic vegetation cover in natural lands?	Simulation type
DGVM ensemble	HYL, LPJ, ORC TRI	Potential natural vegetation everywhere Fixed present-day agricultural cover (Wilson & Henderson-Sellers, 1985)	Yes Yes	Direct-spin up to specified environmental conditions.
	SHE	Fixed present-day agricultural cover (Bartholome et al., 2002)	No	
Climate ensemble	TRI-IMOGEN	Fixed present-day agricultural cover (Armstrong et al., 2016)	Yes	Transient simulations from preindustrial to 2100, followed by an equilibration period under constant forcings
ESM ensemble	HadGEM2-ES, MPI-ESM, LPJ-GUESS	1850–2100 transient land use following RCP 8.5 (Hurtt et al., 2011). Land use fixed after 2100	Yes	
	HadCM3LC	Fixed present-day agricultural cover (Wilson & Henderson-Sellers, 1985)	Yes	

Notes. DGVM, dynamic global vegetation model; ESM, Earth system model.

2006; Wigley, 1995), and the effects on temperature can be seen for the HadGEM2-ES and MPI-ESM ESMS in Figure 1. These feedbacks are particularly strong in the boreal zone, with the stronger local temperature amplification potentially further enhancing the productivity and carbon storage of these regions (Falloon et al., 2012).

3. Results

3.1. Tree Cover

The baseline preindustrial tree cover fraction differs widely between the simulations ($\Delta T = 0$ K in Figure 2a). In the temperate and tropical regions (Figures 2g and 2j) these differences are primarily driven by the simulations from HYL, LPJ, and ORC being for potential natural vegetation, whilst HadGEM2-ES, LPJ-GUESS, and MPI-ESM used 1850 land use at $\Delta T = 0$ K, and thus omitting substantial areas of agricultural land use in temperate and tropical regions. In the boreal region (Figure 2d), however, large intermodel discrepancies in tree cover are apparent that cannot be explained by land use, as agriculture in these regions is limited, and must result from differences in the competition algorithms or definition of tree cover in these high latitudes. The committed global mean tree cover fraction is relatively insensitive to ΔT in most of the DGVMs considered here (Figure 2a); however, this masks substantial regional variation. In the boreal region (Figure 2d), all but one model (LPJ) shows monotonic increases of committed tree cover fraction with ΔT . The very strong positive response of HadCM3LC (black triangles) may be a result of land-atmosphere coupling within the ESM, specifically a localized amplification of warming driven by decreases in surface albedo due to expanding forest cover (Falloon et al., 2012). The other ESMs also see a strong positive response (magenta and blue dots), although only two data points are available. Note that the inclusion of land-use change in these ESM simulations has minimal relevance for the boreal zone where such changes are very limited (Hurt et al., 2011). Temperate tree cover change with ΔT (Figure 2g) is more mixed, with direction of change differing between models, giving a low level of certainty in the projections, even when those models including land-use change (dots) are excluded. This low certainty may stem from different model responses to summer drying (Sitch et al., 2008), with responses of trees to drought a recognized uncertainty in current DGVMs (McDowell et al., 2013; Powell et al., 2013). Tree cover decreases in the temperate region are recorded for all three models that include land-use change (HadGEM2-ES, MPI-ESM, and LPJ-GUESS), but it is not possible to assess the relative contributions of land-use change and vegetation dynamics in driving this decrease. The tropics (Figure 2j) are characterized by a reduction in committed tree cover as ΔT increases above approximately 2 K, for the vast majority of DGVMs. This consistent pattern of decreases may result from several of the DGVMs being run using the HadCM3LC climate patterns, which result in particularly hot and dry tropical regions (Good et al., 2011). Clear decreases in tropical tree fraction with ΔT are not simulated by TRI-MOGEN using multiple climate patterns, whilst LPJ-GUESS, driven by climate from the EC-Earth ESM, would show an increase if land-use change was not simulated (not shown). The ensemble should therefore not be considered to show any robust response for tropical tree fraction changes.

3.2. Productivity and Carbon Storage

Baseline preindustrial productivity and carbon storage ($\Delta T = 0$ K in Figures 2b and 2c) also differ strongly between the models. Relative differences between models do not follow the same pattern as for tree cover, but again large spread in the boreal zone indicates that model structure and parameterization, rather than land-use forcing, drive much of the differences in the absolute baselines. The climate ensemble shows a near-flat response of gross primary productivity (GPP) to ΔT in the temperate zone and a negative response in the tropics (Figure 2), whereas the DGVM and ESM ensembles show much more positive responses. This difference almost certainly derives from the climate ensemble members only differing in strength of climate forcing, whereas the DGVM and ESM ensemble members also differ in $[\text{CO}_2]$. Thus, it can be inferred that most of the GPP increase seen in the DGVM and ESM ensembles in these regions is $[\text{CO}_2]$ -driven. Although the climate ensemble uses only the TRIFFID DGVM, the response of TRI in simulations in which $[\text{CO}_2]$ also increased (pink crosses, blue dots, and black triangles in Figure 2) is consistent with other DGVMs, supporting this interpretation. Conversely, in the boreal zone the slope of the GPP response to ΔT is comparable for all models (Figure 2e), indicating that the GPP increases here are temperature, rather than $[\text{CO}_2]$, driven.

The relationship of committed terrestrial carbon storage with ΔT varies by region. In the tropics, strong changes were simulated for both moderate and strong climate warming, but with some models simulating

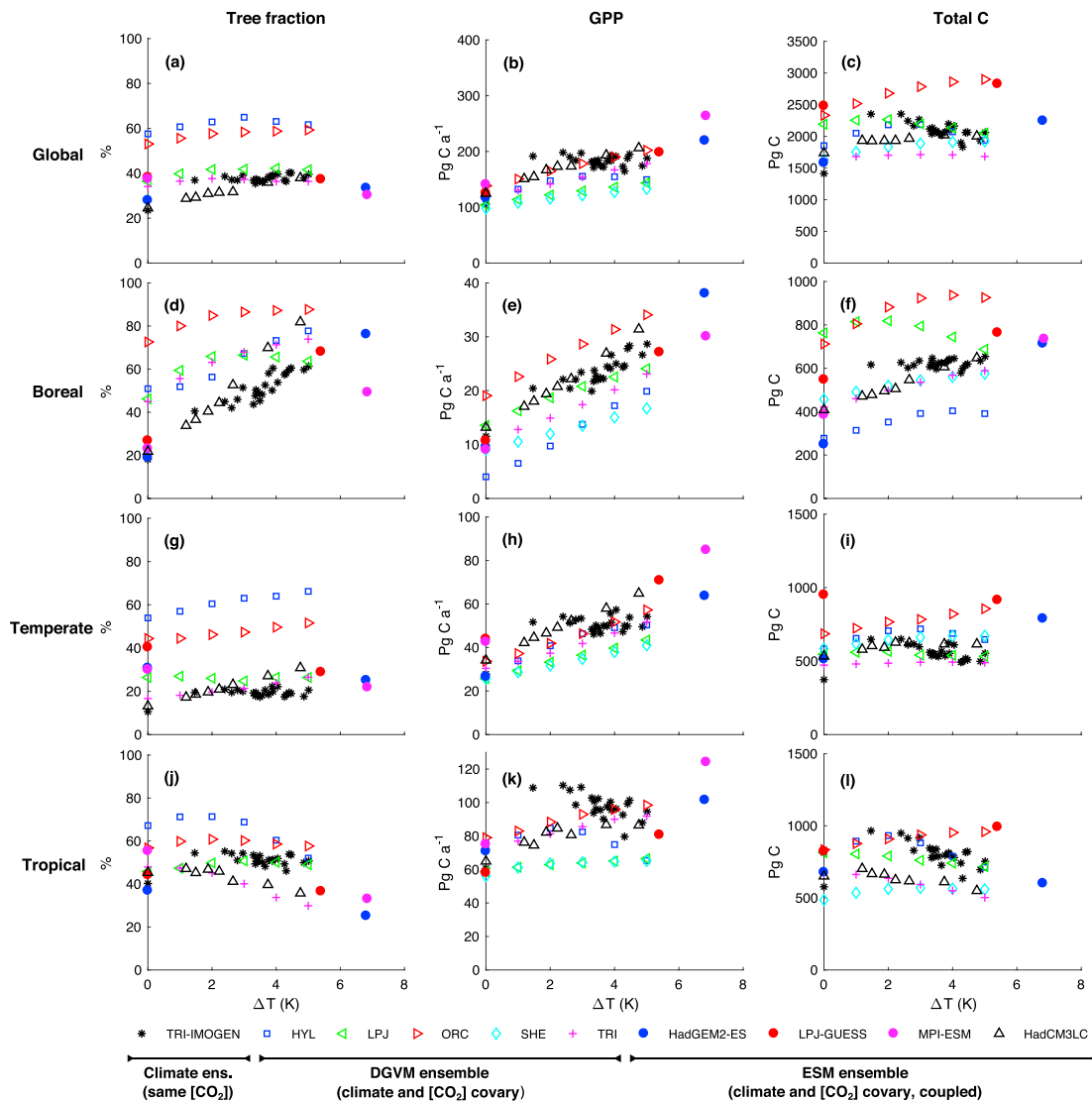


Figure 2. Committed values of tree fraction, gross primary productivity (GPP) and carbon storage as a function of global mean temperature rise above preindustrial (ΔT) for a range of dynamic global vegetation models (DGVMs) and experiment designs. The models represented by filled circles also include dynamic land-use change. Note that y scales vary between panels and that no tree fractions are shown for the SHE simulations as they did not include dynamic vegetation. Very high carbon stocks for MPI-ESM simulations are also not shown. Figure 1 shows the boundary conditions for each simulation type.

stronger losses with increasing ΔT (Table 2). The climate ensemble (Figure 2i, black stars) reveals the response of the TRI DGVM to increasing levels of climate change alone, showing a systematic decrease in tropical carbon storage as ΔT increases. The TRI results from the DGVM ensemble (pink crosses in Figure 2) and also the HadGEM2-ES and HadCM3LC coupled results (blue dots and black triangles), which also use the TRIFFID DGVM, show a similar behavior. That is, tropical carbon storage decreases as ΔT increases, even though these simulations also increase $[CO_2]$ alongside ΔT . However, the rate of decrease of carbon storage with ΔT simulated using TRIFFID is less in the DGVM ensemble than in the climate ensemble, suggesting that the fertilizing effect of increased $[CO_2]$ helps reduce the climate impact on tropical carbon stocks (consistent with Good et al., 2011). The HadGEM2-ES loss of carbon is lower still, in agreement with Good et al. (2013), who showed that HadGEM2-ES predicted less tropical forest dieback than HadCM3LC. Other models behave differently. LPJ-GUESS driven by EC-Earth climate and ORC driven by HadCM3 climate patterns show increasing tropical carbon storage with ΔT across the temperature ranges examined, despite ORC simulations also showing some loss of tropical tree cover. SHE shows an increase

Table 2
Range Across Model Simulations of Difference in Terrestrial Ecosystem Carbon Storage Between Preindustrial and Committed Vegetation States as a Function of ΔT

Region	Variable	Range of stock difference (Pg C)		
		$\Delta T = 2$ K	$\Delta T = 3$ K	$\Delta T = 5$ K
Boreal	Vegetation carbon storage	20 to 95	30 to 118	45 to 201
	Soil carbon storage	2 to 134	-34 to 117 ^a	-155 to 97 ^a
	Total carbon storage	62 to 229	31 to 237	-76 to 256 ^a
Tropical	Vegetation carbon storage	-7 to 222	-47 to 215	-119 to 206
	Soil carbon storage	-26 to 150 ^b	-49 to 124	-121 to 81
	Total carbon storage	-34 to 372 ^b	-77 to 339 ^b	-168 to 176

^aOnly the LPJ model shows a negative carbon stock change in the boreal region. ^bTRI-IMOGEN simulations with moderate climate change but strong $[\text{CO}_2]$ (black stars in Figure 1) give more than double the stock increase of any other simulation.

in tropical carbon for $\Delta T \leq 3$ K, but then a loss thereafter. The mixed response of total carbon storage across models is reflected in the different relative roles of vegetation and soil carbon storage, with five DGVMs showing a vegetation carbon dominance and five a soil carbon dominance (Figure 3b). This uncertainty in the roles of vegetation and soil carbon stocks in the response results in turn from a large uncertainty in changes in the magnitude of GPP increases and in carbon residence times in both soil and vegetation, as shown by the variation in ecosystem residence time (τ_{eco}) and vegetation residence time (τ_{veg}) in Figures 3c and 3d. Carbon storage responses in the temperate region are similarly mixed, although the sign of change for any particular model often differs (Figure S1).

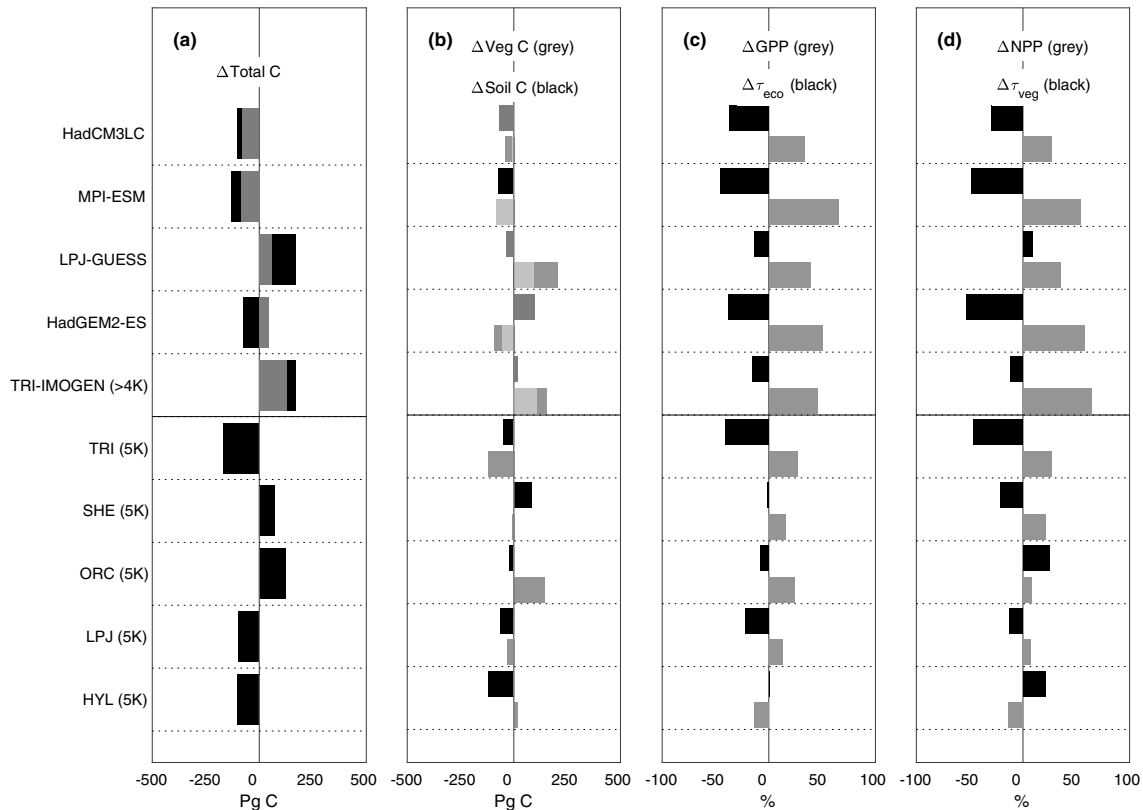


Figure 3. Attribution of changes in tropical (23°S–23°N) terrestrial carbon storage from preindustrial to committed to different pools/processes. (a) Total change in terrestrial carbon storage. (b) Change in vegetation and soil pools. (c) Change in GPP and in τ_{eco} ($\tau_{\text{eco}} = C_{\text{tot}}/\text{GPP}$, where C_{tot} is total ecosystem carbon stock). (d) Change in net primary productivity (NPP) and in τ_{veg} ($\tau_{\text{veg}} = C_{\text{veg}}/\text{NPP}$, where C_{veg} is total vegetation carbon stock). Only model results with $\Delta T > 4$ K and $[\text{CO}_2]$ of at least 700 ppmv are shown to maximize comparability. Results for the climate ensemble are the mean of all models with $\Delta T > 4$ K. The lighter shading in panels a and b for the models from the Earth System Model (ESM) and climate ensembles indicates the stock changes realized by 2100.

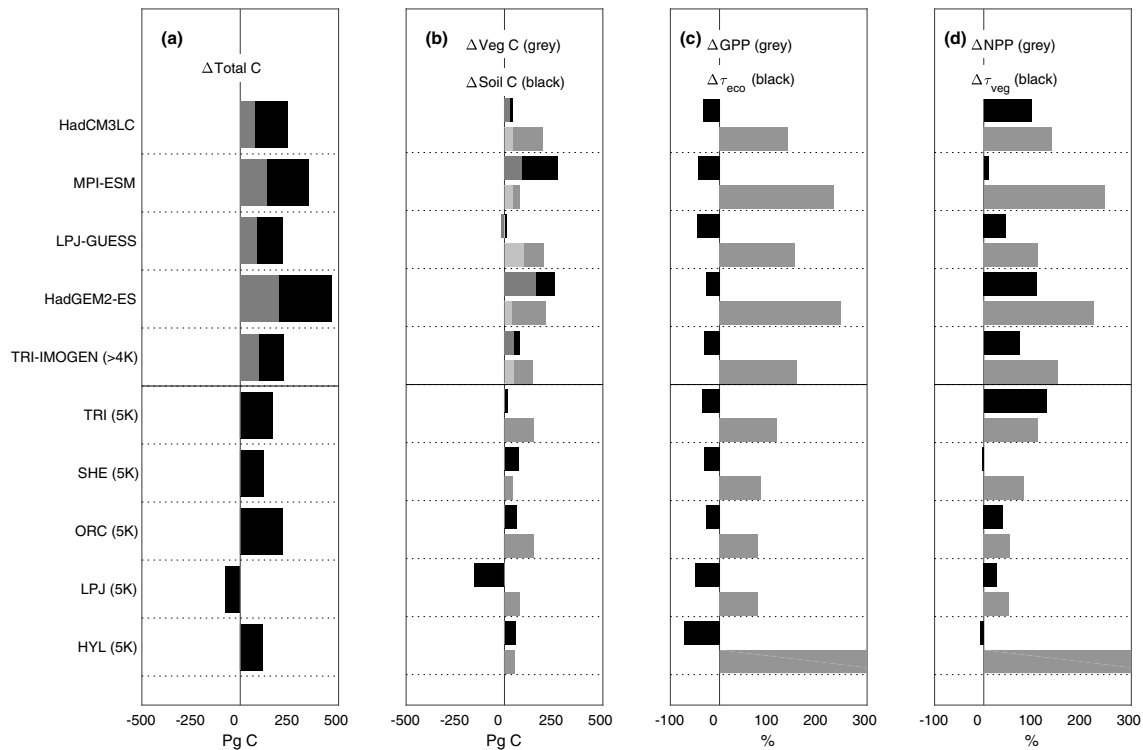


Figure 4. As for Figure 3 except for the boreal region (>55°N).

The boreal zone shows the most consistent set of carbon storage responses to ΔT across the three regions studied, although also a very large intermodel uncertainty in initial carbon stock. Following the strong increases in GPP, all but one model shows increases in total carbon storage as the climate warms (Figures 2 and 4), and these increases can be large even for relatively moderate levels of climate warming (Table 1). The increased carbon storage in vegetation results both from increased GPP and from higher tree cover increasing τ_{veg} , the latter through increasing the fraction of carbon stored in woody tissues, which are long-lived relative to herbaceous vegetation. This behavior is consistent across all models (Figure 4). In all but one of the models, the increased productivity, and thus litter input to soil, also results in an increase in soil carbon storage, outweighing the reductions in τ_{eco} driven by increased temperatures. The exception is LPJ, which exhibits a peak and decline in its tree cover and carbon storage. Sitch et al. (2008) show that in LPJ there is some dieback at the southern edge of the boreal forest due to increased heat-induced mortality of boreal trees. This dieback is accompanied by loss of vegetation carbon, offsetting any increase due to enhanced vegetation growth elsewhere in the boreal zone at high ΔT . This dieback effect is also present in LPJ-GUESS simulations but does not cause carbon storage decreases in the region sums presented here due to the considerable expansion of the boreal forest northwards. In addition, a loss of soil carbon (not seen in the other DGVMs) occurs in LPJ in the higher latitudes across North America and Eurasia. This may be due to the different formulation of soil respiration response to temperature in LPJ, following a modified Arrhenius relationship (Sitch et al., 2003), compared to the Q10-type functions common in other models (Peylin et al., 2005).

3.3. Uncertainty

As shown above, the uncertainty in simulations of changes in carbon storage between preindustrial and committed states is very large (Figures 2–4). The unbalanced nature of the *ensemble of opportunity* used here precludes a formal breakdown of uncertainty (e.g., Hawkins & Sutton, 2009), but comparison of spread along different axes of DGVM and input combinations nonetheless allows an informative attribution of this uncertainty to climate, combined climate and scenario (i.e., climate and $[CO_2]$), and DGVM structural/parameter uncertainties (Figure 5). Comparing five DGVMs with 22 climate states means that small differences in

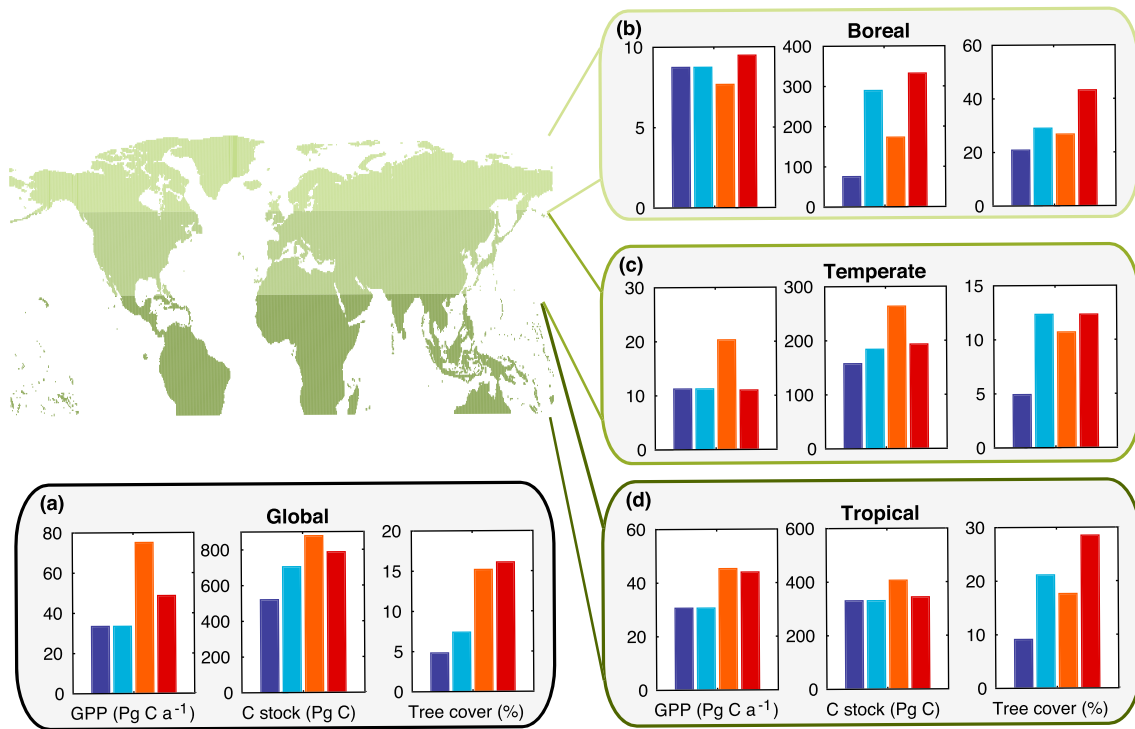


Figure 5. Absolute size of uncertainty ranges in difference of key ecosystem outputs between preindustrial and committed states, calculated as the range of dynamic global vegetation model (DGVM) outputs across different axes of DGVM and input combinations. Climate-based uncertainty (dark blue) is calculated as the range of carbon storage change since preindustrial across all the climate ensemble (constant $[\text{CO}_2]$, variable climate). The combination of climate- and scenario-based uncertainty (light blue) is calculated as the range across all climates and $[\text{CO}_2]$ scenarios from the individual DGVM, which shows the greatest range for this variable. DGVM-based uncertainty at $\Delta T = 2 \text{ K}$ (orange) and 5 K (red) is calculated by taking the range of all models in the DGVM ensemble across a band of $\Delta T \pm 0.5^\circ$ (horizontal transect in Figure 1). Results from the ESM ensemble are excluded to provide a consistent sample of DGVMs for all uncertainty calculations.

uncertainty ranges should not be overinterpreted, but large differences are likely to be indicative, and particularly so in those cases where the spread between the five DGVMs exceeds that between the climatic states (e.g., boreal carbon stock in Figure 5b). Combined climate-and-scenario uncertainty can be artificially inflated here by the differences in DGVM baselines that exist under no climate change. However, where climate-and-scenario uncertainty and climate uncertainty are similar (e.g., for GPP in all regions), this is a strong indicator that uncertainty in climate is at least as important as scenario-based variations in $[\text{CO}_2]$.

At global level, uncertainty in committed GPP and terrestrial carbon storage resulting from differences in DGVM structure (the range across the DGVM ensemble; orange and red bars in Figure 5a) substantially exceeds that of climate uncertainty alone (the range across the climate ensemble; dark blue bar in Figure 5a). This difference is even more marked for tree cover, uncertainty in which is dominated by the choice of DGVM. Notably, the combined climate-and-scenario uncertainty (light blue bar) is relatively similar to climate uncertainty alone, suggesting that uncertainties in CO_2 fertilization effects caused by different levels of $[\text{CO}_2]$ between scenarios are not a dominant component of uncertainty in estimating committed changes in vegetation.

Regional breakdowns differ from the global picture (Figures 5b–5d). In the tropics climate uncertainty and DGVM uncertainty are both large and similar for GPP and carbon stocks and dominate over the effects of varying $[\text{CO}_2]$ in the different scenarios. The exception is tree cover, where climate uncertainty is much less influential than DGVM structural/parameter uncertainty, reflecting a very large uncertainty in the position of the threshold conditions for tree cover loss. The characteristics of temperate uncertainty closely follow tropical; however, the boreal region differs notably. In the boreal region, climate uncertainty has a relatively small effect on carbon storage compared to other drivers. This may reflect that climate-driven changes in ecosystem properties in the boreal region are more sensitive to temperature than to precipitation changes, due to the relaxation of temperature constraints, whereas at lower latitudes precipitation likely plays a larger

role; climate projections show much more uncertainty in precipitation changes than they do for temperature (Collins et al., 2013). DGVM structural/parameter uncertainty for carbon storage is much higher than climate uncertainty and increases markedly with temperature in this region. This follows as absolute differences in productivity and turnover parameterizations in the DGVMs will become more marked as temperature constraints on productivity are lifted. The very large level of combined climate-and-scenario uncertainty for boreal carbon stocks cannot be attributed to the effects of $[\text{CO}_2]$, as $[\text{CO}_2]$ is not a driving force of carbon stock change in the boreal zone (see above; also reflected in the uncertainty in GPP not increasing when scenario uncertainty is included; Figure 5b). This is a consequence of the very large DGVM structural/parameter uncertainty associated with baseline simulation of carbon stocks in this region; the large inter-DGVM differences in baseline stocks and lack of multiple climate simulations for all models means that climate-and-scenario uncertainty for the boreal region cannot be robustly assessed. Overall, the uncertainty in simulated committed boreal carbon stock change is of similar size to that of tropical carbon stocks.

3.4. Post-2100 Changes

Using the simulations in the climate and ESM ensembles, it is possible to assess the relative contributions of change during a typical transient simulation period of preindustrial to 2100 with the change committed to occur post 2100 as a result of pre-2100 changes in environmental boundary conditions. Figure 6 makes this comparison (cf. left versus right columns) for the case of strong climate change (i.e., simulations in which year 2100 $\Delta T > 4$ K). Consistent with the fast response of GPP to a changing environment, GPP increases greatly globally under transient environmental conditions (Figure 6, left) but shows minimal committed change post-2100 (Figure 6, right). Post-2100 changes in GPP are associated with lagged changes in vegetation coverage and are dominated by changes in tropical tree cover, as the majority of global GPP is located in tropical regions.

In contrast to GPP, projected changes in total carbon storage post 2100 are of comparable size to those before 2100, ranging from an additional 87 to 464 Pg C stored prior to 2100, with a further 205–329 Pg C once the biosphere attains its committed state (Figures 6g and 6h). Changes in tree cover fraction are generally relatively small post-2100 in the tropical and temperate zones but can be very large in the boreal zone, at least for the TRIFFID family of models (TRI-IMOGEM, HadGEM2-ES, and HadCM3LC; Figures 6 and S2). Vegetation carbon storage also increases post-2100 for most models, with these changes being a combination of change in carbon storage in existing vegetation and vegetation dynamics. The effect of vegetation dynamics is most marked in the boreal zone, where expansion of tree cover accounts for 84–100% of storage change after 2100 in the TRIFFID family of models, 46% in MPI-ESM, and 18% in LPJ-GUESS (Figure 7). Soil carbon also continues to change strongly after 2100, and the change is overwhelmingly an increase on the global scale, driven especially by increases in the boreal zone. Here the increase in productivity leads to an increase in litter input, which overwhelms the temperature-driven increase in heterotrophic respiration rates. In the tropics respiration rate increases dominate, but the loss of soil carbon in this region is less than the boreal gain for all models.

The importance of rate of change in both soil and vegetation shows very strongly in the ensemble results. The inter-DGVM differences in this lag effect are most clearly seen in the boreal zone, where TRI-IMOGEM and HadGEM2-ES show a relatively small pre-2100 northward expansion of the boreal treeline but a very large committed change in this variable post 2100, whilst LPJ-GUESS and MPI-ESM show a relatively large pre-2100 northward expansion of the treeline, but little change post-2100 (Figure 7). This reflects a very substantial level of uncertainty in the rate at which dynamic changes occur. LPJ-GUESS approaches quasi-equilibrium in its vegetation state approximately 150 years after fixing forcing, and in its soil carbon approximately 200 years after fixing forcing (i.e., the multiannual mean of the rate of change of global carbon pool size was close to zero for these components). For MPI-ESM the equilibration times for vegetation and soil were approximately 100 years and greater than 200 years, respectively. For other models the times required to reach committed vegetation in transient simulations are not available as they were spun-up directly to the committed state, but Jones et al. (2009) showed that the recovery time for vegetation to regrow in the tropics in the TRI model was several times longer than it took to dieback, with only about a tenth of the eventual recovery happening within 100 years. Thus, in addition to large intermodel differences in committed carbon storage (i.e., *carbon storage capacity* in the terminology of Luo et al., 2017) for a given ΔT , a large portion of

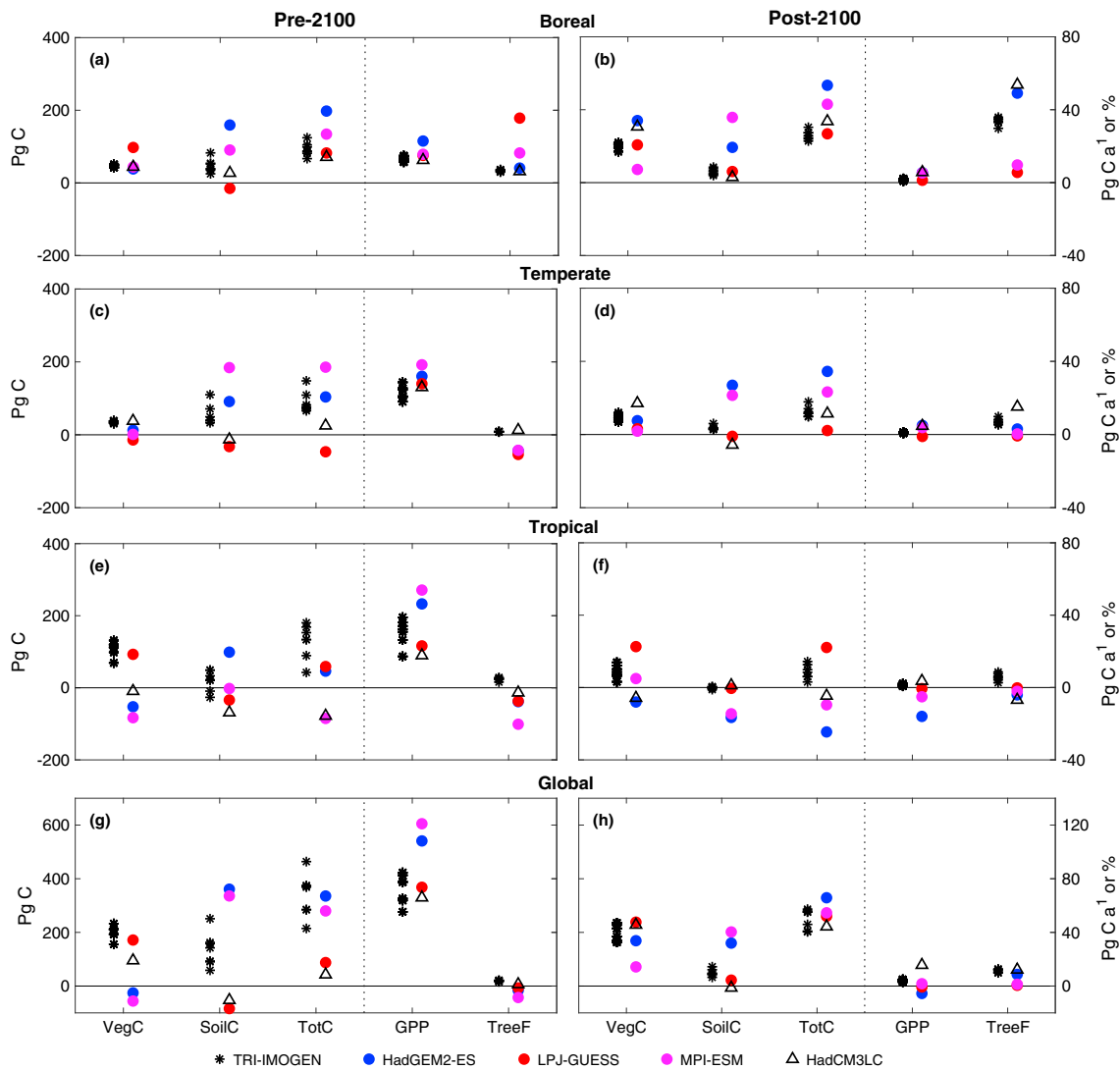


Figure 6. Range of modeled changes in vegetation C, soil C, total C (scale on left axes), GPP (Pg C/a, scale on right axis), and tree cover fraction (% scale on right axis) across simulations with $\Delta T > 4$ K. Only simulations for which both 2100 transient values and committed values are available are shown ($N = 11$, $N_{D_{GVM}} = 5$). The left column (a, c, e, and g) shows the change, which is realized in transient simulations between preindustrial (1850, 1860, or 1900 depending on ensemble member) and 2100; the right column (b, d, f, and h) shows the committed change, which occurs after 2100. Climate and ESM ensembles are plotted in separate columns for clarity.

uncertainty in boreal carbon uptake by 2100 derives from uncertainty in the rate at which that committed storage will be approached.

4. Discussion

In the tropical, and to a lesser extent temperate, regions, the simulations here show that the effect of elevated $[CO_2]$ on GPP is a key driver of any simulated differences in total carbon storage between preindustrial and committed states. This increase in GPP not only leads to increased vegetation carbon stocks but also increases soil carbon inputs, offsetting the effects of temperature-driven increases in heterotrophic respiration (also found by Koven, Chambers, et al., 2015, for ESMs in the CMIP5 model intercomparison project). This highlights both the direct role of CO_2 fertilization and also the improved water-use efficiency of vegetation, which mitigates against the effects of warmer and drier climates in the tropics under climate change. Good et al. (2011) showed that elevated $[CO_2]$ markedly increase the temperature threshold for forest to no-forest transition in HadCM3LC.

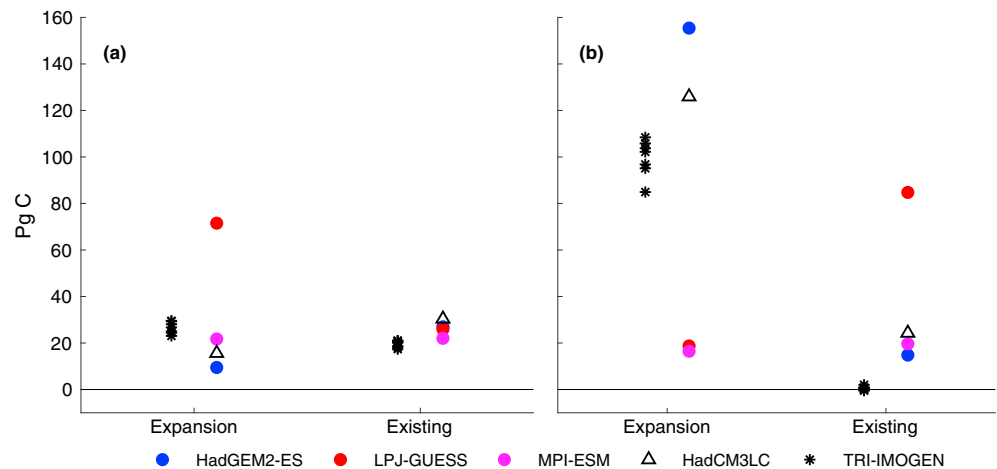


Figure 7. Attribution of the boreal vegetation carbon stock changes between expansion of tree cover (i.e., vegetation dynamics) and changes occurring in areas where the existing vegetation type is unchanged for (a) preindustrial to 2100 and (b) 2100 to committed. The method used to calculate this attribution is given in Appendix B. The blue and red dots overlap for the *existing* column of panel a. Climate and ESM ensembles are plotted in two columns for clarity.

The magnitude of GPP increases projected by this ensemble may be tempered by nutrient limitations, which are not included in any of the DGVMs here. Representation of nitrogen and phosphorus cycling has been shown to pose limitations on the sizes of the CO_2 fertilization effect on terrestrial carbon storage (Goll et al., 2012; Wårlind et al., 2014; Zaehle et al., 2010). However, despite recognized uncertainties in DGVM responses to rising $[\text{CO}_2]$ (e.g., Medlyn et al., 2015; Pugh et al., 2016), the increase of uncertainty in GPP and carbon storage in tropical and temperate committed vegetation is small or nonexistent when $[\text{CO}_2]$ (i.e., scenario) uncertainty is included in addition to climate uncertainty (Figure 5; note that in the boreal region DGVM baseline differences strongly affect this measure, see above). This reflects the crucial role of carbon residence time in governing carbon stocks, and the large uncertainty between models in how residence times are likely to change as a result of environmental change, as recently identified in transient simulations (Friend et al., 2014). Including such nutrient limitations here, and thereby reducing the magnitude of $[\text{CO}_2]$ -induced changes, would be likely to make the climate an even more important driver of uncertainty in committed carbon storage.

Ecosystem state and fluxes in the boreal region are particularly strongly governed by response to climate, rather than $[\text{CO}_2]$. Unlike in the tropics, the DGVM ensemble, which is forced by both increasing $[\text{CO}_2]$ and ΔT , does not have a stronger GPP response than the climate ensemble (Figure 2). Thus, the strong committed boreal carbon uptake projected by the DGVM ensemble is unlikely to be sensitive to uncertainties in the effects of CO_2 fertilization. This may be partially attributable to a weaker CO_2 fertilization effect in cold regions (Hickler et al., 2008), but the dominant factors here are likely to be the relaxation of low-temperature constraints on photosynthesis, the longer growing seasons, and the related northward advance of the boreal treeline. The former processes increase carbon input rate to vegetation and soil, while treeline advance increases the residence time of carbon in vegetation (through a biome-level allocation shift towards wood). Nitrogen limitation may play a role in limiting the boreal carbon uptake simulated here (Zaehle et al., 2015), although this limitation may be more influential for transient carbon uptake rates than for the size of committed carbon stocks due to the possibility of nitrogen accumulation over long timescales. The increase of boreal soil carbon stocks with ΔT in this ensemble is consistent with the results from five ESMs presented by Koven, Chambers, et al. (2015). In contrast, a recent meta-analysis of soil warming observations suggests a strong loss of soil C with temperature in northern soils (Crowther et al., 2016), which is not seen here. However, Crowther et al. were not able to take full account of the accompanying changes in ecosystem productivity which the DGVMs here simulate.

In this model ensemble, changes in vegetation carbon residence time (τ_{veg}) primarily result from changes in the distribution and abundance of plant functional types, that is, vegetation dynamics. It is broadly accepted that vegetation composition is likely to change as climate evolves, but the uncertainty in the processes is very

large. Conceptually, changes in vegetation composition can be split into three categories: (1) loss or change of composition of existing forest vegetation, (2) expansion of trees into previously unforested areas, and (3) changes in composition of nonforest vegetation. The latter is not discussed further here, as its implications for changes in carbon storage are expected to be comparatively small. Categories 1 and 2 are discussed below.

Although it is impossible to evaluate future changes in vegetation composition, aspects of the ensemble response are reflected in other studies. For instance, the change in tree composition from evergreen needle-leaf to deciduous broadleaf forest in the southern boreal region, along with the accompanying loss of vegetation carbon, which is projected by the LPJ and LPJ-GUESS models, was also found by Koven (2013) using a climate analogue method. In the case of both Koven (2013) and the LPJ-GUESS simulations, these losses were driven by the higher levels of disturbance-induced carbon loss associated with the broadleaf forest. Using a climate envelope approach, Zeng et al. (2013) found losses in tropical tree cover, which are broadly consistent with the results of the ensemble here. These qualitative consistencies between differing methods of projection are encouraging, but confidence in such projections is hampered because most DGVMs are evaluated for their ability to capture current vegetation composition, rather than its evolution with changing environmental conditions. Attempts to make such evaluations are stymied by a lack of suitable data; historical records, which could detect composition changes in forests, are either lacking (although some data exist for herbaceous species; e.g., Bertrand et al., 2011), limited to tree lines (e.g., Harsch et al., 2009), or complicated by forest management, whereas the limited spatial coverage of paleo-records necessarily implies relatively high uncertainty (but see Fang et al., 2013). Whether composition exhibits threshold responses to a change in climate, and if so, what these thresholds might be, remains a very active area of research (Abis & Brovkin, 2017; Higgins & Scheiter, 2012; Hirota et al., 2011; Lenton et al., 2008; Scheffer et al., 2001). Suitable data sets for evaluating the response of forest composition to a changing environment are urgently needed and will most likely come from landscape-scale case studies, where the confounding effects of management can be most easily accounted for, and attribution of structural and compositional changes is likely to be most accurate.

The size of the committed boreal carbon sink is very large and results in large part from northward advance of the treeline under warming temperatures. That such a treeline advance would eventually occur under these climatic conditions is supported by known changes in forest distribution with glacial and interglacial cycles (Dyke, 2005; Williams, 2009), and there is evidence suggesting that treelines have advanced over the last century (Harsch et al., 2009). However, the timescale over which such changes will occur is crucial, and the subject of very low confidence, as reflected in the DGVM responses in section 3.4. The rate at which trees can expand into new territory is dependent on existence of appropriate soil (formation of which make take centuries if nothing appropriate already exists) and the presence of seed stock of the expanding species. The latter may have a significant lag due to the time needed for trees to reach reproductive maturity. DGVM simulations to date have omitted explicit representation of these factors. For instance, some DGVMs assume the presence of a base seed stock for all plant functional types in every grid cell, meaning that the treeline change lags climate change only by the necessary time to grow a tree (e.g., LPJ-GUESS and LPJ), whereas the TRIFFID model allocates carbon to growth before vegetation spread, implying very limited seed transport and resulting in a very slow advance. Observations show that seed dispersal distances from trees typically do not exceed a few thousand meters (Grace et al., 2002; Thomson et al., 2011), but the picture is greatly complicated by (a) the occurrence of long-distance seed transport for some species, the likelihood of which is governed by a range of factors such as seed type, animal migration patterns and wind regimes (Nathan et al., 2008), and (b) the scattering of numerous patches of forest, or refugia, across the high latitudes (European Space Agency, 2017). As a result, boreal forest expansion is likely to occur from multiple clusters, rather than as a clean advance of the main forest frontier (e.g., Kharuk et al., 2013), making it challenging to make simple estimates of the rate of boreal treeline advance. More detailed investigation of these processes is needed to inform appropriate parameterizations for DGVMs. Competition with shrubs may slow treeline expansion, as suggested in a recent study of Alaskan treelines (Dial et al., 2016). Fires may also be theorized to limit expansion of the boreal treeline, although both the LPJ and LPJ-GUESS models showed very strong northern forest expansion despite including the effects of fires in their simulations. Some of these challenges have been addressed in landscape- and regional-scale vegetation models (Bocedi et al., 2012; Lischke et al., 2006; Snell, 2014) but require solutions to make them computationally feasible in DGVMs (e.g., Nabel, 2015; Snell et al., 2014). Advancing knowledge and representation of the above processes in DGVMs will be crucial to

ascertain whether large boreal treeline expansion, and the accompanying large carbon sink, is likely to be realized on timescales relevant to current society. As for the existing boreal forest, however, the ultimate size of any boreal carbon sink from an expanding treeline will also be affected by any limits on tree size imposed by nutrient availability, by the disturbance regimes experienced at these high latitudes, and by any canopy structural modifications resulting from the very low solar elevation angle.

The results herein show that a very large, and typically unrecognized, part of uncertainty in future terrestrial carbon uptake is the lagged component of terrestrial change. This is particularly the case for vegetation dynamics and most starkly demonstrated by boreal treeline advance. Although historical changes in land cover are probably dominated by anthropogenic disturbances over the last 1000 years, it has been shown that over the 20th century, dynamic land-cover changes in response to climate change may be equally as large as human interference (Davies-Barnard et al., 2015; Schneck et al., 2015). The results here show that the subsequent, committed changes in tree cover due to vegetation dynamics are larger still. For a strong climate warming scenario, the post-2100 boreal carbon uptake simulated by this ensemble totals 120–267 Pg C, with 16–155 Pg C uptake due to expansion of forest area, that is, vegetation dynamics.

Missing processes—notably the lack of nutrients (Zaehle et al., 2015) and permafrost carbon (Burke et al., 2013)—are often discussed as important omissions from ESM carbon cycle projections (Figure 6.20 in Ciais et al., 2013). However, dynamic vegetation, needed to simulate the boreal carbon uptake effectively, was only included in four ESMs in CMIP5 (Figure 6.38 in Ciais et al., 2013). The results herein show that vegetation dynamics, especially on long timescales, should be included in this discussion too, and its inclusion in ESM projections is clearly of high importance. The magnitude of simulated uptake due to committed vegetation dynamics can be compared to emissions from permafrost soils, which, for a strong warming scenario, have been estimated to be 37–174 Pg C by 2100 based on ESMs (Schuur et al., 2015) and 28–113 Pg C based on a data-constrained approach (Koven, Schuur, et al., 2015). Chadburn et al. (2017) derive data-constrained estimates of permafrost extent lost at a range of global warming levels—in the same way that the results herein are presented in phase space of warming—although they are not able to quantify carbon lost on a given time horizon. Burke et al. (2018) estimate committed permafrost carbon loss in the range 225–345 Pg C over several centuries for a stabilized global temperature rise of 2 °C. Hence, committed vegetation changes represent a missing process potentially as large as, or larger than, the possible loss of carbon from permafrost thawing.

For GPP, ecosystem carbon stocks, and tree fraction, DGVM structural/parameter uncertainty in all regions is at least as large as, or greater than, climate-derived uncertainty (Figure 5). This occurs despite there being considerably more climate ensemble members than DGVM ensemble members. There is no consistent evidence, in the sample of DGVMs here, that the absolute size of DGVM structural/parameter uncertainty increases with temperature above $\Delta T = 2$ K (Figure 5). Previous simulations of transient behavior (Booth et al., 2012; Friend et al., 2014; Jones et al., 2013; Sitch et al., 2008) have also found DGVM uncertainty to be an important factor in committed simulations, as found here. This large importance of DGVM uncertainty in the committed simulations herein corresponds with that seen for transient simulations conducted previously. Although some of the model versions used here are relatively old, in terms of GPP calculations, carbon allocation, and vegetation dynamics, they still provide a representative sample of DGVM technology currently in use for major climate assessments (e.g., CMIP5 and CMIP6). Nonetheless, missing processes may mean that model structural/parameter uncertainty is underestimated. For instance, the uncertainty in vegetation carbon residence time may indeed be even greater than indicated by this ensemble, as there are also open questions as to whether the lifecycle of individual trees may speed up as a result of environmental change (Bugmann & Bigler, 2011; Körner, 2017). On-going efforts to improve representations of vegetation dynamics through models using representations of individual trees and plant-trait variability (e.g., Pavlick et al., 2013; Sakschewski et al., 2016; Scheiter et al., 2013), along with efforts to better understand mortality mechanisms and thresholds (e.g., Anderegg et al., 2015; Brienen et al., 2015; McDowell et al., 2015, 2013), may provide advances in the representation of changes in ecosystem composition, but they are not yet routinely applied at the global scale.

Three of the models in the DGVM ensemble exclude anthropogenic land use (HYL, LPJ, and ORC), explaining the higher absolute values of temperate and tropical tree cover simulated by HYL and ORC (Figure 2). In principle, this means that the total carbon storage changes by these models for these regions are probably an

overestimate, particularly in terms of vegetation carbon change. However, none of these three models shows magnitudes of change in tree fraction or carbon storage that are fundamentally inconsistent with the other models in the ensemble. This caveat does not apply for the assessments of post-2100 change in Figures 6 and 7, in which the DGVM ensemble could not be used, and thus, all models included at least present-day land-use forcing. The use of dynamic land use in HadGEM2-ES, MPI-ESM, and LPJ-GUESS explains at least part of the decrease in temperate and tropical tree cover between preindustrial and committed shown for these models in Figure 2, and their response can only be robustly attributed to vegetation dynamics in the boreal region, where agricultural land use in the applied scenario is low (Figure 12 in Hurtt et al., 2011). However, land-use change cannot explain changes in tree fraction between 2100 and committed states for these models, as land use was held constant after 2100. There is also no evidence that land-use dynamics result in a different character of response of carbon storage in these models, compared to the rest of the ensemble (Figure 6). Although, in principle, soil carbon storage may be affected by land-use legacy emissions after 2100 in these simulations, the expansion of agricultural land in RCP 8.5 over the 21st century is very moderate compared to that in the 20th century (Figure 9a in Hurtt et al., 2011). Thus, legacy emissions are likely to be much smaller than the 40 Pg global emission that has been estimated for 1850–2012 (Pugh et al., 2015).

5. Conclusions

Although simulation of committed states negates the impacts of differences in rate of change between DGVMs, a factor that certainly plays a role in assessments of transient ecosystem state, fundamental differences in productivity, and carbon residence times for a given ΔT results in highly variable estimates of committed carbon storage. The direction of change between preindustrial and committed states diverges strongly in the tropical region, reflecting wide variation in the magnitude of changes in vegetation and ecosystem residence times. However, there is broad consistency in the direction, if not the magnitude, of the carbon storage response in the boreal region, reflecting much more uniform productivity and residence-time responses across the DGVMs. The importance of residence time in determining differences in DGVM response further strengthens the imperative highlighted in recent studies (Friend et al., 2014; Koven, Chambers, et al., 2015) to focus efforts on improving representation of carbon turnover processes in DGVMs, both in vegetation and soil.

The uncertainty in simulated change of boreal carbon stocks between preindustrial and committed states, notwithstanding permafrost, which was not simulated here, was found to be of similar absolute size to that of tropical carbon stocks. Given the substantial and ongoing reduction of actual tropical forest area by land-use change (Klein Goldewijk et al., 2011), reducing its sink potential under climate change (Pugh et al., 2015), constraining potential carbon uptake by boreal vegetation and soils may ultimately prove as important for reducing uncertainty in the long-term state of the global carbon cycle as resolving the mechanistic questions over tropical forest response to environmental change.

Overall, the uncertainty in committed terrestrial carbon uptake resulting from climate and from DGVM structure is on the order of several hundred Pg C across all regions, with the exception of climate-driven uncertainty in the boreal zone. The large magnitude of the uncertainty holds for global mean temperature increases above the preindustrial period of both 2 and 5 K. This poses substantial problem for calculations of budgets of *permissible* emissions consistent with a given level of climate change, as the long-term uncertainties in terrestrial carbon exchange are of the order of the total size of such permissible emission budgets (Jones et al., 2013).

Large committed changes in carbon storage and tree cover fraction are consistently found post-2100. In the boreal zone, committed changes in carbon storage post-2100 are found to be potentially large enough to offset the expected committed carbon losses from thawing permafrost, which have been quantified elsewhere (see above). There are likely temperature limits to such an offset effect, however, as vegetation carbon gain may be saturated at lower ΔT than permafrost loss is exhausted (Schaphoff et al., 2013).

Factorial simulations to directly quantify the contribution of vegetation dynamics (i.e., changes in vegetation composition, particularly treeline advance) were not available here. Such simulations are particularly technically challenging in DGVMs with advanced vegetation dynamics, where competition between plant functional types and the effects of disturbances are fundamental aspects of model structure. Prescribing vegetation cover would lead to neglecting disturbances and modification of the carbon reference state,

complicating comparison of simulations with and without vegetation dynamics. In the absence of factorial simulations, it can be assumed that the simulated changes in committed soil carbon would also be broadly similar in runs without vegetation dynamics. This is a reasonable approximation given that the soil inputs closely mirror net primary productivity, which is not the dominant change post-2100. As such, ESMs without dynamic vegetation would also likely simulate changes in soil carbon similar to shown here. However, without vegetation dynamics, ecosystem commitments would likely show much more limited carbon stock increases, especially in the boreal zone. Therefore, there is a pressing need that vegetation dynamics, in addition to the now widely considered anthropogenic land-cover change, are more routinely represented in coupled ESMs, in order to better understand these natural changes in land cover, particularly in the boreal zone. Furthermore, much more attention needs to be given to the timescales of ecosystem responses. Dynamic vegetation models only offer an advantage over static or equilibrium vegetation distribution methods to the extent that they can realistically simulate the timescales over which changes occur. This study advocates the need for a move away from evaluating DGVMs in terms of their stable vegetation state, toward addressing their ability to capture transient responses.

Appendix A: Simulation Setups

A1. DGVM Ensemble

Following the initial analysis by Jones et al. (2009), a set of off-line vegetation runs were performed using the five DGVMs first analyzed by Sitch et al. (2008). These DGVMs: TRIFFID (TRI), LPJ, SDGVM (SHE), ORCHIDEE (ORC), and HyLand (HYL) were run using the IMOGEN pattern scaling system forced by $[\text{CO}_2]$ (Huntingford et al., 2010; Huntingford & Cox, 2000). They used climate patterns from HadCM3LC (very similar to the climate of HadCM3LC from Jones et al., 2009) and were run to equilibrium at six different global mean temperatures: 0, 1, 2, 3, 4, and 5 K above preindustrial. Corresponding $[\text{CO}_2]$ levels are shown in Figure 1.

A2. CLIMATE Ensemble

The same IMOGEN pattern scaling technique was used to drive the TRIFFID DGVM using climate patterns from 22 global climate models that contributed to CMIP3 (Huntingford et al., 2013). The simulations were driven by $[\text{CO}_2]$ following the SRES A2 scenario. Although these simulations did not set out to attempt to explore different global mean temperature changes within each simulation, the use of results from 22 different climate models as forcing means that there was a large spread in the global temperature change and climate change patterns by 2100.

A3. ESM Ensemble

As part of the EU-FP7 EMBRACE project (www.embrace-project.eu) committed biosphere simulations were made using the models HadGEM2-ES, MPI-ESM, and LPJ-GUESS. The models were initialized with the transient vegetation state, land use, and climate from year 2100, based on the CMIP5 RCP 8.5 simulations. These models were run with fixed radiative forcings and land use until quasi-equilibrium was attained with respect to vegetation dynamics and terrestrial carbon uptake. Due to differences in model formulation and computational demands, the form of these simulations differed between the models, but they were designed to address the same question as systematically as possible.

- *HadGEM2-ES* is an ESM with online coupling of vegetation dynamics and climate. The land surface component of HadGEM2-ES, although essentially a version of the TRIFFID DGVM, cannot be run outside of the ESM. Therefore, the fully coupled system was run for 200 years starting from the year 2100 driven by all RCP 8.5 forcings fixed to the year 2100. Fixing forcings rather than climate meant that climate continued to evolve after 2100 in response to both terrestrial and oceanic changes, with the difference between 2100 and final ΔT indicated by the small and large circles in Figure 1. For a period of this simulation vegetation dynamics were accelerated so that the vegetation cover would quickly come into equilibrium with the climate forcings of 2100.
- *MPI-ESM-LR* is also an ESM (Giorgetta et al., 2013) with online coupling of vegetation dynamics and climate (Brovkin et al., 2009; Reick et al., 2013). It was used to make a 200-year transient simulation under fixed

radiative forcings and land cover, initialized at the end of the r1i1p1 RCP 8.5 simulation. As for HadGEM2-ES, actual climate was allowed to evolve after 2100 in response to terrestrial and oceanic changes. Vegetation dynamics were not artificially accelerated.

- *LPJ-GUESS* is an off-line DGVM (Ahlström et al., 2012; Smith et al., 2001), which was run here using climate data from the EC-Earth ESM v2.3. A 251-year transient simulation was initialized in 1850 and run with transient climate, $[CO_2]$, and land-cover change until 2100. The model was then run for a further 300 years with $[CO_2]$ and land cover fixed as for year 2100 of the r6i1p1 RCP 8.5 EC-Earth simulation submitted to CMIP5. In order to provide variability necessary for the fire module, climate post-2100 was provided by repeating temperature, precipitation, and solar radiation from the period 2071–2100. The temperature data for this period were detrended using linear regression and the mean temperature set to that indicated by the regression for the year 2100.

The ESM ensemble additionally includes the simulations with HadCM3LC presented by Jones et al. (2009).

Appendix B: Attribution of Vegetation Carbon Changes

Attribution of changes in vegetation carbon storage between changes in existing vegetation and changes in tree cover was carried out for each model grid cell as follows. Calculating the vegetation carbon per fraction tree cover (CvegF) for each grid cell in the baseline year (i.e., preindustrial state or 2100 depending on whether pre-2100 or post-2100 changes are being calculated).

$$CvegF = Cveg_0 / TF_0,$$

where $Cveg_0$ is vegetation carbon stock in the baseline year and TF_0 is fractional tree cover in the baseline year. Calculating the change in tree fraction,

$$\Delta TF = TF_{end} - TF_0,$$

where TF_{end} is the fractional tree cover in the final state (i.e., 2100 or committed), and thus calculating the change in vegetation carbon due to change of tree cover,

$$\Delta Cveg_{TF} = \Delta TF \times CvegF$$

The change in vegetation carbon due to environmental change was calculated as a residual,

$$\Delta Cveg_{env} = \Delta Cveg - \Delta Cveg_{TF},$$

with the fraction of $\Delta Cveg_{env}$ in vegetation that existed in the baseline year being

$$\Delta Cveg_{env,base} = \Delta Cveg_{env} \times \min(TF_0 / TF_{end}, 1.0).$$

Acknowledgments

This analysis was carried out for the European Commission's Seventh Framework Program grant agreement 282672 (EMBRACE). C. D. J., C. B., and E. R. were supported by the Joint UK BEIS/Defra Met Office Hadley Centre Climate Programme (GA01101). This work was supported, in part, by the German Federal Ministry of Education and Research (BMBF), through the Helmholtz Association and its research program ATMO. Peter Levy is thanked for providing the Hyland simulations. This is paper number 32 of the Birmingham Institute of Forest Research. The model output underlying this analysis is provided as supporting information to this paper. The authors declare no financial conflicts of interest.

References

- Abis, B., & Brovkin, V. (2017). Environmental conditions for alternative tree-cover states in high latitudes. *Biogeosciences*, *14*, 511–527. <https://doi.org/10.5194/bg-14-511-2017>
- Ahlström, A., Schurgers, G., Arneth, A., & Smith, B. (2012). Robustness and uncertainty in terrestrial ecosystem carbon response to CMIP5 climate change projections. *Environmental Research Letters*, *7*, 44008. <https://doi.org/10.1088/1748-9326/7/4/044008>
- Anderegg, W. R. L., Flint, A., Huang, C., Flint, L., Berry, J. A., Davis, F. W., et al. (2015). Tree mortality predicted from drought-induced vascular damage. *Nature Geoscience*, *8*, 367–371. <https://doi.org/10.1038/ngeo2400>
- Armstrong, E., Valdes, P., House, J., & Singarayer, J. (2016). The role of CO_2 and dynamic vegetation on the impact of temperate land-use change in the HadCM3 Coupled Climate Model. *Earth Interactions*, *20*, 10. <https://doi.org/10.1175/EI-D-15-0036.1>
- Avitabile, V., Herold, M., Heuvelink, G. B. M., Simon, L., Phillips, O. L., Asner, G. P., et al. (2016). An integrated pan-tropical biomass map using multiple reference datasets. *Global Change Biology*, *22*, 1406–1420. <https://doi.org/10.1111/gcb.13139>
- Bartholome, E., Belward, A. S., Achard, F., Bartalev, S., Carmona-Morex, C., Eva, H., et al. (2002). GLC 2000 Global land cover mapping for the year 2000. Project status November 2002. European Commission, Joint Research Centre.
- Bertrand, R., Lenoir, J., Piedallu, C., Riofrio-Dillon, G., de Ruffray, P., Vidal, C., et al. (2011). Changes in plant community composition lag behind climate warming in lowland forests. *Nature*, *479*, 517–520. <https://doi.org/10.1038/nature10548>
- Bocedi, G., Pe'er, G., Heikkinen, R. K., Matsinos, Y., & Travis, J. M. (2012). Projecting species' range expansion dynamics: Sources of systematic biases when scaling up patterns and processes. *Methods in Ecology and Evolution*, *3*, 1008–1018.
- Booth, B. B. B., Chris, D. J., Mat, C., Ian, J. T., Peter, M. C., Stephen, S., et al. (2012). High sensitivity of future global warming to land carbon cycle processes. *Environmental Research Letters*, *7*, 24002. <https://doi.org/10.1088/1748-9326/7/2/024002>

- Brienen, R. J. W., Phillips, O. L., Feldpausch, T. R., Gloor, M., Baker, T. R., Lloyd, J., et al. (2015). Long-term decline of the Amazon carbon sink. *Nature*, 519, 344–348. <https://doi.org/10.1038/nature14283>
- Brovkin, V., Raddatz, T., Reick, C. H., Claussen, M., & Gayler, V. (2009). Global biogeophysical interactions between forest and climate. *Geophysical Research Letters*, 36, L07405. <https://doi.org/10.1029/2009GL037543>
- Bugmann, H., & Bigler, C. (2011). Will the CO₂ fertilization effect in forests be offset by reduced tree longevity? *Oecologia*, 165, 533–544. <https://doi.org/10.1007/s00442-010-1837-4>
- Burke, E. J., Chadburn, S. E., Huntingford, C., Jones, C. D. (2018). CO₂ loss by permafrost thawing implies additional emissions reductions to limiting warming to 1.5 or 2 °C. *Environmental Research Letters* 13(2), 024024, 9.
- Burke, E. J., Jones, C. D., & Koven, C. D. (2013). Estimating the permafrost-carbon climate response in the CMIP5 climate models using a simplified approach. *Journal of Climate*, 26, 4897–4909. <https://doi.org/10.1175/JCLI-D-12-00550.1>
- Chadburn, S. E., Burke, E. J., Cox, P. M., Friedlingstein, P., Hugelius, G., & Westerman, S. (2017). A observation-based constraint on permafrost loss as a function of global warming. *Nature Climate Change*, 7, 340–344.
- Ciais, P., Sabine, C., Bala, G., Bopp, L., Brovkin, V., Canadell, J., et al. (2013). Carbon and other biogeochemical cycles. In T. F. Stocker et al. (Eds.), *Climate change 2013: The physical science basis. Contribution of Working Group I to the Fifth Assessment Report of the Intergovernmental Panel on Climate Change* (pp. 465–570). Cambridge, United Kingdom and New York, NY, USA: Cambridge University Press.
- Clark, D. B., Mercado, L. M., Sitch, S., Jones, C. D., Gedney, N., Best, M. J., et al. (2011). The Joint UK Land Environment Simulator (JULES), model description—Part 2: Carbon fluxes and vegetation dynamics. *Geoscientific Model Development*, 4, 701–722. <https://doi.org/10.5194/gmd-4-701-2011>
- Collins, M., Knutti, R., Arblaster, J., Dufresne, J.-L., Fichefet, T., Friedlingstein, P., et al. (2013). Long-term climate change: Projections, commitments and irreversibility. In *Climate change 2013: The physical science basis. Contribution of Working Group I to the Fifth Assessment Report of the Intergovernmental Panel on Climate Change* (pp. 1029–1136). Cambridge: Cambridge University Press.
- Cramer, W., Bondeau, A., Woodward, F. I., Prentice, I. C., Betts, R. A., Brovkin, V., et al. (2001). Global response of terrestrial ecosystem structure and function to CO₂ and climate change: Results from six dynamic global vegetation models. *Global Change Biology*, 7, 357–373. <https://doi.org/10.1046/j.1365-2486.2001.00383.x>
- Crowther, T. W., Todd-Brown, K. E. O., Rowe, C. W., Wieder, W. R., Carey, J. C., & AI, E. (2016). Quantifying global soil carbon losses in response to warming. *Nature*, 540, 104–108. <https://doi.org/10.1038/nature20150>
- Davies-Barnard, T., Valdes, P. J., Singarayer, J. S., Wiltshire, A. J., & Jones, C. D. (2015). Quantifying the relative importance of land cover change from climate and land use in the representative concentration pathways. *Global Biogeochemical Cycles*, 29, 842–853. <https://doi.org/10.1002/2014GB004949>
- Dial, R. J., Smeltz, T. S., Sullivan, P. F., Rinas, C. L., Timm, K., Geck, J. B., et al. (2016). Shrubline but not treeline advance matches climate velocity in montane ecosystems of south-central Alaska. *Global Change Biology*, 22, 1841–1856. <https://doi.org/10.1111/gcb.13207>
- Dunne, J. P., John, J. G., Shevliakova, S., Stouffer, R. J., Krasting, J. P., Malyshev, S. L., et al. (2013). GFDL's ESM 2 global coupled climate-carbon earth system models. Part II: Carbon system formulation and baseline simulation characteristics. *Journal of Climate*, 26, 2247–2267. <https://doi.org/10.1175/JCLI-D-12-00150.1>
- Dyke, A. S. (2005). Late Quaternary vegetation history of Northern North America based on pollen, macrofossil, and faunal remains. *Géographie physique et Quaternaire*, 59, 211–262. <https://doi.org/10.7202/014755ar>
- European Space Agency (2017). ESA CCI Land Cover dataset (v 1.6.1) [WWW Document]. URL <https://www.esa-landcover-cci.org/?q=node/169> (accessed 6.29.17).
- Eyring, V., Bony, S., Meehl, G. A., Senior, C. A., Stevens, B., Stouffer, R. J., et al. (2016). Overview of the Coupled Model Intercomparison Project Phase 6 (CMIP6) experimental design and organization. *Geoscientific Model Development*, 9, 1937–1958.
- Falloon, P. D., Dankers, R., Betts, R. A., Jones, C. D., Booth, B. B. B., & Lambert, F. H. (2012). Role of vegetation change in future climate under the A1B scenario and a climate stabilization scenario, using the HadCM3C Earth system model. *Biogeosciences*, 9, 4739–4756. <https://doi.org/10.5194/bg-9-4739-2012>
- Fang, K., Morris, J. L., Salonen, J. S., Miller, P. A., Renssen, H., & Sykes, M. T. (2013). How robust are Holocene treeline simulations? A model-data comparison in the European Arctic treeline region. *Journal of Quaternary Science*, 28, 595–604. <https://doi.org/10.1002/jqs.2654>
- Friend, A. D., Lucht, W., Rademacher, T. T., Kerbin, R., Betts, R., Cadule, P., et al. (2014). Carbon residence time dominates uncertainty in terrestrial vegetation responses to future climate and atmospheric CO₂. *Proceedings of the National Academy of Sciences of the United States of America*, 111, 3280–3285. <https://doi.org/10.1073/pnas.1222477110>
- Giorgetta, M. A., Jungclaus, J., Reick, C. H., Legutke, S., Bo, M., Brovkin, V., et al. (2013). Climate and carbon cycle changes from 1850 to 2100 in MPI-ESM simulations for the Coupled Model Intercomparison Project phase 5. *Journal of Advances in Modeling Earth Systems*, 5, 572–597. <https://doi.org/10.1002/jame.20038>
- Goll, D. S., Brovkin, V., Parida, B. R., Reick, C. H., Kattge, J., Reich, P. B., et al. (2012). Nutrient limitation reduces land carbon uptake in simulations with a model of combined carbon, nitrogen and phosphorus cycling. *Biogeosciences*, 9, 3547–3569. <https://doi.org/10.5194/bg-9-3547-2012>
- Good, P., Jones, C., Lowe, J., Betts, R., Booth, B., & Huntingford, C. (2011). Quantifying environmental drivers of future tropical forest extent. *Journal of Climate*, 24, 1337–1349. <https://doi.org/10.1175/2010JCLI3865.1>
- Good, P., Jones, C., Lowe, J., Betts, R., & Gedney, N. (2013). Comparing tropical forest projections from two generations of Hadley Centre Earth System Models, HadGEM2-ES and HadCM3LC. *Journal of Climate*, 26, 495–511. <https://doi.org/10.1175/JCLI-D-11-00366.1>
- Grace, J., Berninger, F., & Nagy, L. (2002). Impacts of climate change on the tree line. *Annals of Botany*, 90, 537–544. <https://doi.org/10.1093/aob/mcf222>
- Hare, B., & Meinshausen, M. (2006). How much warming are we committed to and how much can be avoided? *Climatic Change*, 75, 111–149. <https://doi.org/10.1007/s10584-005-9027-9>
- Harsch, M. A., Hulme, P. E., McGlone, M. S., & Duncan, R. P. (2009). Are treelines advancing? A global meta-analysis of treeline response to climate warming. *Ecology Letters*, 12, 1040–1049. <https://doi.org/10.1111/j.1461-0248.2009.01355.x>
- Hawkins, E., & Sutton, R. (2009). The potential to narrow uncertainty in regional climate projections. *Bulletin of the American Meteorological Society*, 1095–1107. <https://doi.org/10.1175/2009BAMS2607.1>
- Hickler, T., Prentice, I. C., Smith, B., & Sykes, M. T. (2006). Implementing plant hydraulic architecture within the LPJ dynamic global vegetation model. *Global Ecology and Biogeography*, 15, 567–577. <https://doi.org/10.1111/j.1466-822x.2006.00254.x>
- Hickler, T., Smith, B., Prentice, I. C., Mjöfors, K., Miller, P., Arneeth, A., et al. (2008). CO₂ fertilization in temperate FACE experiments not representative of boreal and tropical forests. *Global Change Biology*, 14, 1531–1542. <https://doi.org/10.1111/j.1365-2486.2008.01598.x>
- Higgins, S. I., & Scheiter, S. (2012). Atmospheric CO₂ forces abrupt vegetation shifts locally, but not globally. *Nature*, 488, 209–212. <https://doi.org/10.1038/nature11238>

- Hirota, M., Holmgren, M., Van Nes, E. H., & Scheffer, M. (2011). Global resilience of tropical forest. *Science* (80-), 334, 232–235. <https://doi.org/10.1126/science.1210657>
- Huntingford, C., Booth, B. B. B., Sitch, S., Gedney, N., Lowe, J. A., Liddicoat, S. K., et al. (2010). IMOGEN: An intermediate complexity model to evaluate terrestrial impacts of a changing climate. *Geoscientific Model Development*, 3, 679–687. <https://doi.org/10.5194/gmd-3-679-2010>
- Huntingford, C., & Cox, P. M. (2000). An analogue model to derive additional climate change scenarios from existing GCM simulations. *Climate Dynamics*, 16, 575–586.
- Huntingford, C., Zelazowski, P., Galbraith, D., Mercado, L. M., Sitch, S., Fisher, R., et al. (2013). Simulated resilience of tropical rainforests to CO₂-induced climate change. *Nature Geoscience*, 6, 268–273. <https://doi.org/10.1038/ngeo1741>
- Hurttt, G. C., Chini, L. P., Frolking, S., Betts, R. A., Feddema, J., Fischer, G., et al. (2011). Harmonization of land-use scenarios for the period 1500–2100: 600 years of global gridded annual land-use transitions, wood harvest, and resulting secondary lands. *Climatic Change*, 109, 117–161. <https://doi.org/10.1007/s10584-011-0153-2>
- Jones, C., Lowe, J., Liddicoat, S., & Betts, R. (2009). Committed terrestrial ecosystem changes due to climate change. *Nature Geoscience*, 2, 484–487. <https://doi.org/10.1038/ngeo555>
- Jones, C., Robertson, E., Arora, V., Friedlingstein, P., Shevliakova, E., Bopp, L., et al. (2013). Twenty-first-century compatible co2 emissions and airborne fraction simulated by cmip5 Earth system models under four representative concentration pathways. *Journal of Climate*, 26, 4398–4413. <https://doi.org/10.1175/JCLI-D-12-00554.1>
- Kharuk, V. I., Ranson, K. J., Im, S. T., Oskorbin, P. A., Dvinskaya, M. L., Ovchinnikov, D. V., et al. (2013). Tree-line structure and dynamics at the northern limit of the Larch Forest: Anabar Plateau, Siberia, Russia. Arctic, Antarctic, Alp. *Reserach*, 45, 526–537.
- Klein Goldewijk, K., Beusen, A., Van Drecht, G., & De Vos, M. (2011). The HYDE 3.1 spatially explicit database of human-induced global land-use change over the past 12,000 years. *Global Ecology and Biogeography*, 20, 73–86. <https://doi.org/10.1111/j.1466-8238.2010.00587.x>
- Körner, C. (2017). A matter of tree longevity. *Science* (80-), 355, 130–131.
- Koven, C. D. (2013). Boreal carbon loss due to poleward shift in low-carbon ecosystems. *Nature Geoscience*, 6, 452–456. <https://doi.org/10.1038/ngeo1801>
- Koven, C. D., Chambers, J. Q., Georgiou, K., Knox, R., Riley, W. J., Arora, V. K., et al. (2015). Controls on terrestrial carbon feedbacks by productivity versus turnover in the CMIP5 Earth System Models. *Biogeosciences*, 12, 5211–5228. <https://doi.org/10.5194/bg-12-5211-2015>
- Koven, C. D., Schuur, E. A. G., Schädel, C., Bohn, T. J., Burke, E. J., Chen, G., et al. (2015). A simplified, data-constrained approach to estimate the permafrost carbon-climate feedback. *Philosophical Transactions of the Royal Society A*, 373. <https://doi.org/10.1098/rsta.2014.0423>
- Lenton, T. M., Held, H., Kriegler, E., Hall, J. W., Lucht, W., Rahmstorf, S., et al. (2008). Tipping elements in the Earth's climate system. *Proceedings of the National Academy of Sciences of the United States of America*, 105, 1786–1793. <https://doi.org/10.1073/pnas.0705414105>
- Lischke, H., Zimmermann, N. E., Bolliger, J., Rickebusch, S., & Löffler, T. J. (2006). TreeMig: A forest-landscape model for simulating spatio-temporal patterns from stand to landscape scale. *Ecological Modelling*, 199, 409–420.
- Luo, Y., Shi, Z., Lu, X., Xia, J., Liang, J., Jiang, J., et al. (2017). Transient dynamics of terrestrial carbon storage: Mathematical foundation and its applications. *Biogeosciences*, 14, 145–161. <https://doi.org/10.5194/bg-14-145-2017>
- Martin, G. M., Bellouin, N., Collins, W. J., Culverwell, I. D., Halloran, P. R., Hardiman, S. C., et al. (2011). The HadGEM2 family of Met Office Unified Model climate configurations. *Geoscientific Model Development*, 4, 723–757. <https://doi.org/10.5194/gmd-4-723-2011>
- McDowell, N. G., Coops, N. C., Beck, P. S. A., Chambers, J. Q., Gangodagamage, C., Hicke, J. A., et al. (2015). Global satellite monitoring of climate-induced vegetation disturbances. *Trends in Plant Science*, 20, 114–123. <https://doi.org/10.1016/j.tplants.2014.10.008>
- McDowell, N. G., Fisher, R. a., Xu, C., Domec, J. C., Hölltä, T., Mackay, D. S., et al. (2013). Evaluating theories of drought-induced vegetation mortality using a multimodel-experiment framework. *The New Phytologist*, 200, 304–321. <https://doi.org/10.1111/nph.12465>
- Medlyn, B. E., Zaehle, S., De Kauwe, M. G., Walker, A. P., Dietze, M. C., Hanson, P. J., et al. (2015). Using ecosystem experiments to improve vegetation models. *Nature Climate Change*, 5, 528–534. <https://doi.org/10.1038/nclimate2621>
- Nabel, J. E. (2015). Upscaling with the dynamic two-layer classification concept (D2C): TreeMig-2 L, an efficient implementation of the forest-landscape model TreeMig. *Geoscientific Model Development*, 8(11), 3563–3577.
- Nathan, R., Schurr, F. M., Spiegel, O., Steinitz, O., Trakhtenbrot, A., & Tsoar, A. (2008). Mechanisms of long-distance seed dispersal. *Trends in Ecology & Evolution*, 23, 638–647. <https://doi.org/10.1016/j.tree.2008.08.003>
- Neilson, R. P., Prentice, I. C., Smith, B., Kittel, T., & Viner, D. (1998). Simulated changes in vegetation distribution under global warming. In R. T. Watson, M. C. Zinyowera, & R. H. Moss (Eds.), *Regional impacts of climatic change: An assessment of vulnerability. A special report of the Intergovernmental Panel on Climate Change (IPCC) Working Group II* (pp. 439–456). Cambridge, United Kingdom: Cambridge University Press.
- Pavlick, R., Drewry, D. T., Bohn, K., Reu, B., & Kleidon, A. (2013). The Jena Diversity- dynamic global vegetation model (JeDi-DGVM): A diverse approach to representing terrestrial biogeography and biogeochemistry based on plant functional trade-offs. *Biogeosciences*, 10, 4137–4177. <https://doi.org/10.5194/bg-10-4137-2013>
- Peylin, P., Bousquet, P., Le Quééré, C., Sitch, S., Friedlingstein, P., Mckinley, G., et al. (2005). Multiple constraints on regional CO₂ flux variations over land and oceans. *Global Biogeochemical Cycles*, 19, GB1011. <https://doi.org/10.1029/2003GB002214>
- Piao, S., Sitch, S., Ciais, P., Friedlingstein, P., Peylin, P., Wang, X., et al. (2013). Evaluation of terrestrial carbon cycle models for their response to climate variability and to CO₂ trends. *Global Change Biology*, 19, 2117–2132. <https://doi.org/10.1111/gcb.12187>
- Port, U., Brovkin, V., & Claussen, M. (2012). The influence of vegetation dynamics on anthropogenic climate change. *Earth System Dynamics*, 3, 233–243. <https://doi.org/10.5194/esd-3-233-2012>
- Powell, T., Galbraith, D., Christoffersen, B., Harper, A., Imbuzeiro, H. M. A., Rowland, L., et al. (2013). Confronting model predictions of carbon fluxes with measurements of Amazon forests subjected to experimental drought. *The New Phytologist*, 200, 350–364. <https://doi.org/10.1111/nph.12390>
- Pugh, T. A. M., Arneth, A., Olin, S., Ahlström, A., Bayer, A. D., Goldewijk, K. K., et al. (2015). Simulated carbon emissions from land-use change are substantially enhanced by accounting for agricultural management. *Environmental Research Letters*, 10, 124008. <https://doi.org/10.1088/1748-9326/10/12/124008>
- Pugh, T. A. M., Müller, C., Arneth, A., Haverd, V., & Smith, B. (2016). Key knowledge and data gaps in modeling the influence of CO₂ concentration on the terrestrial carbon sink. *Journal of Plant Physiology*, 203, 3–15. <https://doi.org/10.1016/j.jplph.2016.05.001>
- Reick, C. H., Raddatz, T., Brovkin, V., & Gayler, V. (2013). Representation of natural and anthropogenic land cover change in MPI-ESM. *Journal of Advances in Modeling Earth Systems*, 5, 459–482. <https://doi.org/10.1002/jame.20022>
- Sakschewski, B., Von Bloh, W., Boit, A., Poorter, L., Peña-claros, M., Heinke, J., et al. (2016). Resilience of Amazon forests emerges from plant trait diversity. *Nature Climate Change*. <https://doi.org/10.1038/NCLIMATE3109>
- Schaphoff, S., Heyder, U., Ostberg, S., Gerten, D., Heinke, J., & Lucht, W. (2013). Contribution of permafrost soils to the global carbon budget. *Environmental Research Letters*, 8, 014026. <https://doi.org/10.1088/1748-9326/8/1/014026>

- Scheffer, M., Carpenter, S., Foley, J. A., Folke, C., & Walker, B. (2001). Catastrophic shifts in ecosystems. *Nature*, *413*, 591–596. <https://doi.org/10.1038/35098000>
- Scheiter, S., Langan, L., & Higgins, S. I. (2013). Next-generation dynamic global vegetation models: Learning from community ecology. *The New Phytologist*, *198*, 957–969.
- Schneck, R., Reick, C. H., Pongratz, J., & Gayler, V. (2015). The mutual importance of anthropogenically and climate-induced changes in global vegetation cover for future land carbon emissions in the MPI-ESM CMIP5 simulations. *Global Biogeochemical Cycles*, *29*, 1816–1829. <https://doi.org/10.1002/2014GB004959>
- Schuur, E. A. G., McGuire, A. D., Schädel, C., Grosse, G., Harden, J. W., Hayes, D. J., et al. (2015). Climate change and the permafrost carbon feedback. *Nature*, *520*, 171–179.
- Sitch, S., Friedlingstein, P., Gruber, N., Jones, S. D., Murray-Tortarolo, G., Ahlström, A., et al. (2015). Recent trends and drivers of regional sources and sinks of carbon dioxide. *Biogeosciences*, *12*, 653–679. <https://doi.org/10.5194/bg-12-653-2015>
- Sitch, S., Huntingford, C., Gedney, N., Levy, P. E., Lomas, M., Piao, S. L., et al. (2008). Evaluation of the terrestrial carbon cycle, future plant geography and climate-carbon cycle feedbacks using five dynamic global vegetation models (DGVMs). *Global Change Biology*, *14*, 2015–2039. <https://doi.org/10.1111/j.1365-2486.2008.01626.x>
- Sitch, S., Smith, B., Prentice, I. C., Arneth, A., Bondeau, A., Cramer, W., et al. (2003). Evaluation of ecosystem dynamics, plant geography and terrestrial carbon cycling in the LPJ dynamic global vegetation model. *Global Change Biology*, *9*, 161–185. <https://doi.org/10.1046/j.1365-2486.2003.00569.x>
- Smith, B., Prentice, I. C., & Sykes, M. T. (2001). Representation of vegetation dynamics in the modeling of terrestrial ecosystems: Comparing two contrasting approaches within European climate space. *Global Ecology and Biogeography*, *10*, 621–637. <https://doi.org/10.1046/j.1466-822X.2001.t01-1-00256.x>
- Smith, T. M., & Shugart, H. H. (1993). The transient response of terrestrial carbon storage to a perturbed climate. *Nature*, *361*, 523–526.
- Snell, R. S. (2014). Simulating long-distance seed dispersal in a dynamic vegetation model. *Global Ecology and Biogeography*, *23*, 89–98.
- Snell, R. S., Huth, A., Nabel, J. E. M. S., Bocedi, G., Travis, J. M. J., Gravel, D., et al. (2014). Using individual based forest models to simulate species range shifts. *Ecography*, *37*, 1184–1197.
- Thomson, F. J., Moles, A. T., Auld, T. D., & Kingsford, R. T. (2011). Seed dispersal distance is more strongly correlated with plant height than with seed mass. *Journal of Ecology*, *99*, 1299–1307. <https://doi.org/10.1111/j.1365-2745.2011.01867.x>
- Turner, M., Beer, C., Santoro, M., Carvalhais, N., Wutzler, T., Schepaschenko, D., et al. (2014). Carbon stock and density of northern boreal and temperate forests. *Global Ecology and Biogeography*, *23*, 297–310. <https://doi.org/10.1111/geb.12125>
- Wärlind, D., Smith, B., Hickler, T., & Arneth, A. (2014). Nitrogen feedbacks increase future terrestrial ecosystem carbon uptake in an individual-based dynamic vegetation model. *Biogeosciences*, *11*, 6131–6146. <https://doi.org/10.5194/bgd-11-151-2014>
- Wigley, T. M. L. (1995). Global-mean temperature and sea level consequences of greenhouse gas concentration stabilization. *Geophysical Research Letters*, *22*, 45–48. <https://doi.org/10.1029/94GL01011>
- Williams, J. W. (2009). Quaternary vegetation distribution. In V. Gornitz (Ed.), *Encyclopedia of paleoclimatology and ancient environments* (pp. 856–862). Netherlands: Kluwer Academic Publishers. <https://doi.org/10.1126/science.206.4418.550>
- Wilson, M. F., & Henderson-Sellers, A. (1985). A global archive of land cover and soils data for use in general circulation climate models. *Journal of Climatology*, *5*, 119–143.
- Zaehle, S., Friedlingstein, P., & Friend, A. D. (2010). Terrestrial nitrogen feedbacks may accelerate future climate change. *Geophysical Research Letters*, *37*, L01401. <https://doi.org/10.1029/2009GL041345>
- Zaehle, S., Jones, C. D., Houlton, B., Lamarque, J.-F., & Robertson, E. (2015). Nitrogen availability reduces CMIP5 projections of twenty-first-century land carbon uptake. *Journal of Climate*, *28*, 2494–2511. <https://doi.org/10.1175/JCLI-D-13-00776.1>
- Zeng, Z., Piao, S., Chen, A., Lin, X., Nan, H., Li, J., et al. (2013). Committed changes in tropical tree cover under the projected 21st century climate change. *Scientific Reports*, *3*, 1951. <https://doi.org/10.1038/srep01951>
- Zhu, D., Peng, S. S., Ciais, P., Viovy, N., Druel, A., Kageyama, M., et al. (2015). Improving the dynamics of Northern Hemisphere high-latitude vegetation in the ORCHIDEE ecosystem model. *Geoscientific Model Development*, *8*, 2263–2283. <https://doi.org/10.5194/gmd-8-2263-2015>